Analysis of Continuous-time Robust Control Models using Finite, Sampled, Experimental Data

Report

Author(s):
Smith, Roy; Dullerud, Geir

Publication date:
1995

Permanent link:
https://doi.org/10.3929/ethz-b-000672706

Originally published in:
Center for Control Engineering & Computation. Technical Report CCEC-95-0313

Published: Roy Smith and Geir Dullerud, "Analysis of Continuous-time Robust Control Models using Finite, Sampled, Experimental Data," *University of California, Santa Barbara, Center for Control Engineering & Computation,* Technical report: CCEC-95-0313, 1995.
DOI: https://doi.org/10.3929/ethz-b-000672706

Analysis of Continuous-time Robust Control Models using Finite, Sampled, Experimental Data

Roy Smith* Geir Dullerud†

CCEC–95–0313

Abstract

The application of robust control theory requires applicable models containing unknown, bounded, perturbations and unknown, bounded input signals. Model validation is a quantitative means of assessing the applicability of a given model with respect to experimental data.

This paper develops a theoretical framework, and a computational solution, for the model validation problem in the case where the model, including unknown perturbations and signals, is given in the continuous time, yet the experimental datum is a finite, sampled, signal. The continuous nature of the unknown components is treated directly with a sampled data lifting theory. This gives results which are valid for any sample period and any datum length. Explicit calculation of whether sufficient data for invalidation has been obtained arises naturally in this framework. A common class of robust control models is treated in both open- and closed-loop and yields a convex matrix optimization problem. A simulation, and an experimental, example illustrate the approach.

*Dept. of Electrical & Computer Engineering, University of California, Santa Barbara, CA 93106.

†Electrical Engineering, Caltech 116–81, Pasadena, CA, 91125.

Contents

1 Introduction

The underlying motivation for this work comes from the problem of designing a control system for a physical plant. Almost all design methods require a model representing the plant behavior, and furthermore, the model must be compatible with the design approach. The more recent approaches, particularly robust control, require models which cannot be provided by the standard identification techniques (meaning those described by Ljung [1]). This mismatch has hindered the application of robust control and has led to an increased interest in the problem of modeling uncertain systems.

Robust control models contain, in addition to unknown additive noise, bounded perturbations which can be used to describe unmodeled dynamics. See for example, [2, 3, 4, 5, 6, 7] and the references therein. This is a powerful formulation as such dynamics can be destabilizing under feedback. Linear models in which all uncertainty is described by additive noise do not have the ability to predict the destabilizing effects of uncertainty. The model perturbations are not entirely arbitrary and are described as unknown elements of a specified class. In the work presented here we will concentrate on the H_∞/structured singular value framework.

Standard identification techniques currently do not lead to suitable bounds on the perturbations, although some work is heading in this direction. The work of Goodwin, Ninness and Salgado [8, 9, 10] or Hjalmarsson and Ljung [11] begins to investigate this area. The resulting model formulations do not match those used for the design methodology we are considering here.

The area of identification in H_∞, developed by Parker and Bitmead [12] and Helmicki, Jacobson and Nett [13, 14], with additional work by Mäkilä and Partington [15, 16] and Gu and Khargonekar [17], focuses on developing algorithms to provide a robust control model, in the H_∞ framework. In attempting to identify a model in this framework, assumptions are usually required to provide a well posed problem. A priori H_∞ perturbation bounds are often assumed and data is taken and analyzed in order to provide a compatible model, meeting the bounds with a small amount of additive noise. The full generality of the robust control framework cannot yet be handled and the perturbation bound is not derived from the experimental data.

Several research groups are investigating iterative identification/design methodologies in a robust control framework. Such approaches do not yet have a rigorous theoretical backing. We note the work of Zang, Bitmead and Gevers [18]; Lee et al. [19]; and, in the area of H_∞ based schemes, Schrama and Van den Hof [20, 21]

Model validation is the converse side of the identification problem — given a system model, which includes assumptions, we would like to assess whether the model is consistent with experimental observations. No assumptions are made about the nature of the physical system. Rather, measurements are taken, and the assumption that the model describes the system is directly tested. In a robust control context model validation is equivalent to asking whether or not there exists an unknown vector valued signal and an unknown perturbation, satisfying the specified assumptions and accounting for the input-output datum. This is the question that we address in this report.

Model validation for least squares/stochastic models has been applied for some time and Ljung [1] gives an overview of model validation in the standard identification framework. In the robust control framework there is no identification methodology that generates models, guaranteed to be consistent with the observed data. Robust control models are often obtained from a combination of standard identification approaches and ad-hoc estimates of perturbation bounds. We also note that validation is with respect to a single experiment. It is not possible to validate a model from a finite amount of data; however a single datum can invalidate a model. We will maintain the customary practice of referring to this procedure as model validation, although the term model invalidation is clearly more descriptive. Our formal results will be presented in terms of invalidation conditions.

The model validation problem was posed and solved for frequency domain data and general H_∞/μ models by Smith and Doyle [22, 23]. Krause et al. [24] studied a similarly motivated problem: the implications of test data on determining stability margins. The frequency domain data requirement is not the easiest to apply to experiments and Poolla et al. [25] considered the model validation problem for discrete-time models with time-domain experimental data. Their formulation applied to a more restricted, although still common, class of perturbations. Zhou and Kimura [26] have considered a similar problem and addressed the issue of identifying certain system parameters in this framework.

In this paper we investigate a more experimentally motivated model validation problem for H_∞/μ robust control models. The system, and the given model, are in the continuous time domain. A known input is applied and measurements of the system output are obtained by sampling. We explicitly account for the continuous nature of the model, unknown perturbations, and unknown noise. This approach therefore gives a closer connection to the physical model than we would obtain by discretizing the model and attempting to validate a discrete time approximation of the model. The consideration of the continuous time intersample effects also allows us to consider the problem for any sample rate without requiring bandlimited assumptions on the signals in the system. The chosen sample rate clearly affects the validation experiment outcome and this is brought out in the approach taken here; slow sample rates may not generate enough data to invalidate a model.

We consider robust control models with the standard additive or multiplicative perturbations both in open- and closed-loop experiments. The paradigm we use here builds on the purely discrete-time work of Poolla et al. [27] and Zhou and Kimura [26]. The continuous-time nature of the unknown perturbations and unknown signals is handled by applying the sampled data lifting framework developed by Bamieh, Pearson, Francis and Tannenbaum [28, 29]. See also the related work of Yamamoto [30]. This allows us to characterize the effects of the infinite dimensional continuous-time parts of the system in a finite dimensional manner. From this we develop a matrix optimization formulation for the solution to the model validation problem. In the perturbation framework considered here this reduces to a convex optimization problem.

The outline of the paper is as follows. Section 2 gives the required theoretical background. The lifting theory is outlined in this section and the model framework is formally introduced. Section 3 presents the main results of the paper. The experimental configuration is detailed and the appropriate model validation problem is defined. A framework is developed and applied to the solution of the model validation problem. This leads to a convex optimization problem and the details of this are outlined in Section 4. Section 5 presents a simulation based example which is helpful in clarifying the application of the theory. An experimental application, illustrating some of the engineering aspects, is presented in Section 6. We conclude with a discussion of the results in Section 7.

Portions of this work have been submitted to the IEEE Transactions on Automatic Control and the International Journal of Robust and Nonlinear Control.

2 Theoretical Background

This section provides the required background on robust control models, the general model validation problem, and the sampled-data lifting theory. All of these areas are detailed elsewhere so we only provide an outline and introduce our notation.

2.1 Signal Spaces and Lifting

This section defines the basic mathematical objects we will use in the sequel, and introduces a useful lifting operation. The lifting operation presented is from [28, 29]. The symbol $\mathcal{R}$ will denote the real numbers, and $\mathcal{Z}^+$ the non-negative integers. Define the Hilbert space $L_2^m[0,\infty)$ consisting of functions, mapping the interval $[0,\infty)$ to $\mathcal{R}^m$, that have finite energy:

$$L_2[0,\infty) := \left\{ u : \ \|u\|_2^2 := \int_0^{+\infty} |u(t)|_2^2 \, dt < +\infty \right\},$$

where $|\cdot|_2$ is the Euclidean norm. Usually, we will just write L_2 when the interval of definition and Euclidean dimension are clear.

We next define a particular class of sequence spaces. Suppose $\mathcal{H}$ is a Hilbert space with norm $\|\cdot\|_{\mathcal{H}}$; we define the space $l_2(\mathcal{H})$ to be the sequences mapping $\mathcal{Z}^+$ to $\mathcal{H}$ that are square summable. Namely,

$$l_2(\mathcal{H}) := \left\{ \psi : \|\psi\|_2^2 := \sum_{k=0}^{\infty} \|\psi_k\|_{\mathcal{H}}^2 < \infty \right\}.$$

Note from the above definitions that $\|\cdot\|_2$ is context dependent. Also, observe that when $\mathcal{H} = \mathcal{R}^m$ we have the usual space of square summable sequences.

Given two Hilbert spaces $\mathcal{H}_1$ and $\mathcal{H}_2$, and a linear operator $Q : \mathcal{H}_1 \to \mathcal{H}_2$, we define the induced norm of Q to be

$$\|Q\|_{\mathcal{H}_1 \to \mathcal{H}_2} := \sup_{u \in \mathcal{H}_1, u \neq 0} \frac{\|Qu\|_{\mathcal{H}_2}}{\|u\|_{\mathcal{H}_1}}.$$

When the induced norm on Q is clear from the context we simply write $\|Q\|$, suppressing the dependence on $\mathcal{H}_1$ and $\mathcal{H}_2$. This defines the norm topology. We will also require the weak* (or weak operator) topology; a sequence Q_k of bounded operators $\mathcal{H}_1 \to \mathcal{H}_2$ converges to Q in this topology if

$$\langle x, Q_k y \rangle_{\mathcal{H}_2} \overset{k\to\infty}{\longrightarrow} \langle x, Qy \rangle_{\mathcal{H}_2} \qquad \text{for all } x \in \mathcal{H}_1 \text{ and } y \in \mathcal{H}_2.$$

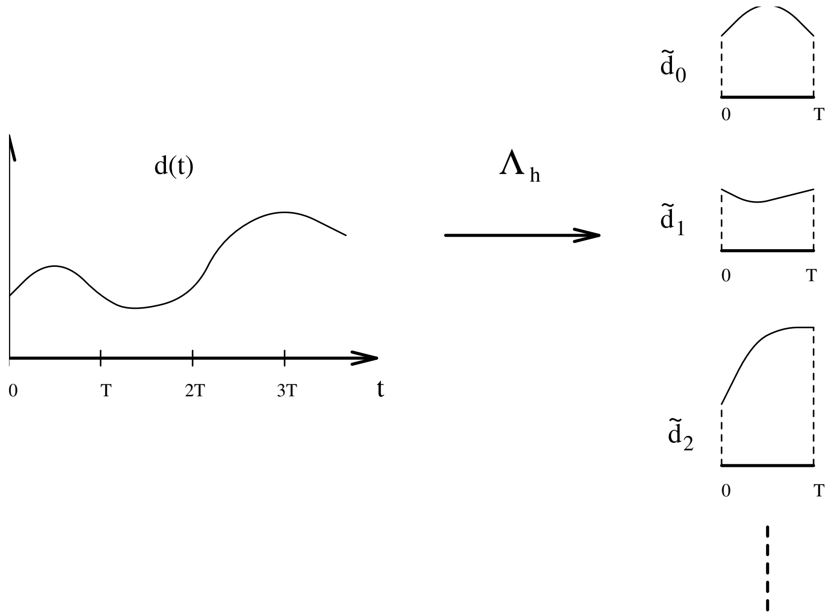

Figure 1: Lifting Operation

We recall a useful property of this topology: if Q_k is a uniformly bounded sequence of operators, then there exists an operator Q, so that a subsequence Q_{k_j} converges weak* to Q. See, for example, [31] for this compactness result.

We now proceed to define a lifting operator that will be used extensively in this work. To start, define $L_2[0,\, h)$, for $h > 0$, to be the space of square integrable functions mapping $[0,\, h)$ to $\mathcal{R}^n$; the compression of $L_2[0,\, \infty)$. Our goal is now to define an isomorphism between $L_2[0,\, \infty)$ and $l_2(L_2[0,\, h)\,)$. Define $\Lambda_h : L_2[0,\, \infty) \to l_2(L_2[0,\, h)\,)$ to be the map that takes $d \in L_2[0, \infty)$ to the sequence $\tilde{d}_k = (\Lambda_h d)_k \in L_2[0,\, h)$ via,

$$(\tilde{d}_k)(\tau) := d(\tau + kh) \qquad \text{for } k \geqslant 0,\ \tau \in [0,\, h). \tag{1}$$

The effect of this mapping is intuitively shown in Figure 1. Clearly Λ_h^{-1} is well-defined, and $\|\Lambda_h\| = \|\Lambda_h^{-1}\| = 1$, so Λ_h is an isometric isomorphism.

As a general rule, a signal $d \in L_2[0, \infty)$ will be denoted in a standard math script (e.g: d or $d(t)$). Its associated lifted signal will be denoted by $\tilde{d}$, or $\tilde{d}_k$, or $\tilde{d}_k(\tau)$ depending upon context. In the following we will often associate lifted signals, $\tilde{d}$, with vectors sequences in l_2 and in this case the vectors are denoted by $\bar{d}$ or $\bar{d}_k$ as is appropriate.

2.2 Perturbation Types

This section is devoted to defining the perturbation classes we will be dealing with in the paper. The two main dynamical properties we will be focusing on are causality and time-variation.

To start, define the truncation operator $\Pi_\tau : L_2[0,\infty) \to L_2[0,\tau)$ for each $\tau > 0$ by $(\Pi_\tau u)(t) = u(t)$ for $t \leqslant \tau$. An operator on $L_2[0,\infty)$ is *causal* if

$$\Pi_\tau \Delta \Pi_\tau^* \Pi_\tau = \Pi_\tau \Delta \qquad \text{for all } \tau > 0.$$

Note that Π_τ^* naturally inserts $L_2[0,\tau)$ into $L_2[0,\infty)$, and that $\Pi_\tau^*\Pi_\tau$ is a projection operator.

Also, define the shift operator $\Xi_\tau : L_2[0,\infty) \to L_2[0,\infty)$ for each $\tau \geqslant 0$ via $(\Xi_\tau u)(t) = u(t-\tau)$ for $t \geqslant \tau$ and zero otherwise. Then Δ is defined to be *linear time-invariant (LTI)* if

$$\Xi_\tau \Delta = \Delta \Xi_\tau \qquad \text{for all } \tau > 0.$$

Related to these definitions we have *h-anticipatory* and *h-periodicity*: given $h > 0$, an operator Δ is said to be h-anticipatory if,

$$\Pi_{kh} \Delta \Pi_{kh}^* \Pi_{kh} = \Pi_{kh} \Delta$$

for all integers $k \geqslant 1$; the operator is h-periodic if,

$$\Xi_h \Delta = \Delta \Xi_h.$$

The term h-anticipatory refers to the fact that the output of the operator may depend upon the input by up to time h in advance. In other words, if Δ is h-anticipatory $\Xi_h \Delta$ is causal.

Similarly, in discrete time we define the truncation operator π_n, mapping $l_2(\mathcal{H})$ to $(\bigoplus_{k=0}^{n} \mathcal{H})$, by $(\pi\psi)_k = \psi_k$ if $0 \leqslant k \leqslant n$ and zero otherwise. The discrete shift operator $\zeta : l_2(\mathcal{H}) \to l_2(\mathcal{H})$ is defined by $(\zeta\psi)_k = \psi_{k-1}$ for $k \geqslant 1$ and $(\zeta\psi)_0 = 0$. An operator Δ on $l_2(\mathcal{H})$ is defined to be causal if,

$$\pi_k \Delta = \pi_k \Delta \pi_k^* \pi_k \qquad \text{for all } k \geqslant 0.$$

and LTI if,

$$\zeta \Delta = \Delta \zeta.$$

In the sequel we will be particularly concerned with a special type of existence problem for operators; we now describe the discrete time setup for this problem and present some preliminary results. Given two finite, Hilbert space valued sequences,

$$(u_0, \dots, u_n) \quad \text{and} \quad (y_0, \dots, y_n)$$

in the orthogonal sum $\bigoplus_{k=0}^{n} \mathcal{H}$, what is the operator Δ of smallest norm satisfying

$$y^e = \Delta u^e,$$

where u^e and y^e are any sequences in $l_2(\mathcal{H})$ that satisfy

$$\begin{aligned} u^e &= (u_0, \dots, u_n, u_{n+1}, \dots) \\ y^e &= (y_0, \dots, y_n, y_{n+1}, \dots). \end{aligned}$$

That is, we want to specify the first $n+1$ entries of an input-output pair. Observe that if Δ is causal the above condition is equivalent to $y = \pi_n \Delta \pi_n^* u$.

We now state two so-called extension theorems, which solve such existence problems under different constraints on the time variation of Δ.

Proposition 1 *Suppose that u and y are in $\bigoplus_{k=0}^{n} \mathcal{H}$. Then there exists a causal operator Δ on $l_2(\mathcal{H})$ satisfying,*

$$y = \pi_n \Delta \pi_n^* u, \qquad \textit{with } \|\Delta\| \leqslant 1, \tag{2}$$

if and only if,

$$\sum_{k=0}^{l} \|y_k\|_{\mathcal{H}}^2 \leqslant \sum_{k=0}^{l} \|u_k\|_{\mathcal{H}}^2 \qquad \textit{for all } 0 \leqslant l \leqslant n.$$

In the proposition statement, (2) expresses the fact that we want to specify $n+1$ entries of the input-output pair. The result above is formally equivalent to one found in [27], the only difference being that here $\mathcal{H}$ can be infinite dimensional; we therefore omit the proof.

The perturbation in the preceding proposition gives conditions for the existence of a causal operator; the next result provides similar conditions, but for causal, LTI perturbations; a more restrictive class.

Proposition 2 *Suppose that* u *and* y *are in* $\bigoplus_{k=0}^{n} \mathcal{H}$*. Then there exists an LTI, causal, operator* Δ *on* $l_2(\mathcal{H})$ *satisfying,*

$$y = \pi_n \Delta \pi_n^* u, \qquad \text{with } \|\Delta\| \leqslant 1, \tag{3}$$

if and only if,

$$Y^*Y \leqslant U^*U \qquad \text{on } \mathcal{R}^n$$

where U *and* Y *map* $\mathcal{R}^{n+1}$ *to* $\bigoplus_{k=0}^{n} \mathcal{H}$ *and are defined by*

$$Y := \begin{bmatrix} y_0 & 0 & 0 & \cdots & 0 \\ \vdots & y_0 & 0 & \cdots & 0 \\ y_{n-1} & \cdots & y_0 & \cdots & 0 \\ y_n & y_{n-1} & \cdots & \ddots & y_0 \end{bmatrix} \quad U := \begin{bmatrix} u_0 & 0 & 0 & \cdots & 0 \\ \vdots & u_0 & 0 & \cdots & 0 \\ u_{n-1} & \cdots & u_0 & \cdots & 0 \\ u_n & u_{n-1} & \cdots & \ddots & u_0 \end{bmatrix}. \tag{4}$$

This proposition is an operator valued version of the classic Caratheodory interpolation theorem; see, for example, [32, p. 195] for a proof of this operator generalization.

2.3 H_∞/μ Robust Control Models

We now introduce, using the formalism of Doyle [3], the generic robust control model. This is given by the input-output relationship,

$$y = [P_{21}\Delta(I - P_{11}\Delta)^{-1}P_{12} + P_{22}]\begin{bmatrix} w \\ u \end{bmatrix},$$

where Δ is an unknown, bounded perturbation. The signal w is unknown and assumed to belong to some specified signal set. In considering model validation, both the input u and output y are known. Measurement noise on either is modeled as a scaled component of w. Note that for some perturbation Δ, the term $(I - P_{11}\Delta)$ may not be invertible. This feature allows the framework to model perturbations that are potentially destabilizing under feedback. This particular model formulation is referred to as a linear fractional transformation (LFT) and will be abbreviated to,

$$y = \mathrm{F_u}(P, \Delta)\begin{bmatrix} w \\ u \end{bmatrix}.$$

This is a useful framework as interconnections of LFTs are simply larger LFTs.

The uncertainty about the system is captured by the assumptions on w and Δ. As P can be scaled, Δ is taken to be unity norm bounded. Additional structure may also be imposed; multiple perturbations at various locations within a complex system can be modeled as a block diagonal Δ. Refer to Packard and Doyle [33] for detail on the more general representations.

In the H_∞/μ framework specific assumptions are applied to P, Δ and w. The model, P, is assumed to be linear, time-invariant (LTI). The unknown signal, w, is of unity bounded energy (or power), i.e. $w \in BL_2$. For vector-valued w, the spatial norm is assumed to be the Euclidean norm. The perturbation, Δ, has an assumed bound: $\|\Delta\|_{L_2 \to L_2} \leqslant 1$; and it is usually also assumed that Δ is LTI. Analysis and design is also possible for Δ assumed to be linear time-varying (LTV) [34, 35, 36] and our results address this case also.

2.4 Model Validation for H_∞/μ Models

It is assumed that an LTI model, P, is given and an experimental datum (y,u) is under consideration. The robust control model validation problem can be formulated as follows.

The Model Validation Problem: *Given a robustly stable model P, and an experimental datum (u, y), does there exist (w,Δ), $w \in BL_2$, $\|\Delta\|_{L_2 \to L_2} \leqslant 1$, such that*

$$y = \mathrm{F_u}(P, \Delta)\begin{bmatrix} w \\ u \end{bmatrix}. \tag{5}$$

This simply asks the question "is there an element of the model set and an element of the unknown input signal set such that the observed datum is produced exactly"? Note that using the LFT framework makes this formulation general. It can equally well apply to closed-loop and MIMO systems.

Solving the model validation problem amounts to assessing whether or not a given robust control model is consistent with a given experimental datum. No assumptions are made about the physical system — rather, we are assessing, with respect to a particular datum, the assumptions that we will subsequently use for design. This procedure is applicable to the identification of robust control models as it gives a means of rejecting inappropriate models. It is also useful in the evaluation of simplified models and in the area of fault detection under closed-loop operation [37].

The initial work of Smith and Doyle [22, 23] considered the experimental datum, (u,y), to be available in the frequency domain. The work of Poolla et al. [25], and Zhou and Kimura [26] considers a discrete time datum, (u_k,y_k) and a discrete-time model, $P(z)$. We now look at the more experimentally motivated case where model, P, and the underlying system, are in the continuous time domain and experimental datum consists of a known input, $u(t)$, and an output, y_k, obtained by sampling.

The next section formulates the model validation problem in a sampled data framework and gives our main results.

3 Sampled Data Model Validation

We will consider the model validation problem for continuous time models and sampled measurements. This model assumes that the unknown signals, w, are in BL_2 and that the perturbation, $\Delta : L_2 \to L_2$, with $\|\Delta\|_{L_2 \to L_2} \leqslant 1$. The experimental datum is obtained by applying a known input, $u(t)$, to the system and sampling the output, $y(t)$, via a sampler. The datum therefore consists of a finite number of vector valued samples.

The framework we present has no restrictions on either the number of samples taken or the sampling period. However, in practice we find that using a long sample period, or taking too few samples, may give an experimental datum that does not invalidate the model; whereas sampling the same experiment at a higher rate would have invalidated the model. These ideas will be explicitly detailed subsequently.

Significant computational issues arise depending on the manner in which the perturbation enters the system. For additive or multiplicative perturbations, with disturbances modeled at the output, a convex, non-differentiable optimization problem results. This is also true for additive and multiplicative models in a sampled-data feedback loop. While the framework presented here can be applied to the most general LFT models, the resulting optimization problem is not necessarily convex. The discussion of the next section will explicitly clarify which cases lead to convex optimization problems.

For notational simplicity, we will consider the case where there are $n + 1$ output samples, sampled with period h. Irregularly spaced samples,

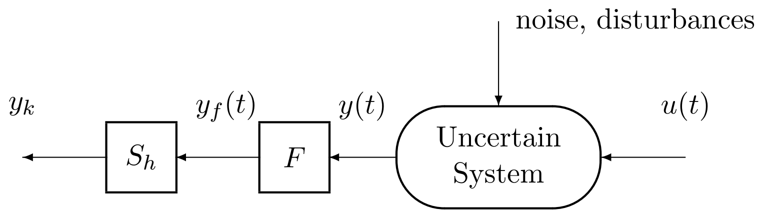

Figure 2: Schematic of the physical experimental configuration

input/output vectors of unequal length, and a variety of other input hold functions, are handled by straightforward, if tedious, modifications of the details provided here.

3.1 Experimental Configuration

The experiment, with the physical system, is illustrated conceptually in Figure 2. The system F represents an anti-aliasing filter, preceding an ideal sampler (of period h), S_h, which maps functions to sequences by

$$(S_h\, y)_k = y(kh), \quad k = 0, 1, \ldots .$$

The input to the system, $u(t)$, is assumed to be known, and is considered as part of the datum. We assume that $u(t) = 0$ for $t < 0$. The available datum is $(y_k,u(t))$, $k = 0, 1, \ldots, n$, and $t \in [0, nh]$.

This paper will focus on robust control models having the structure illustrated in Figure 3, where P_w, P_v, P_z and P_y are all finite dimensional, stable, LTI operators; P_w and P_v are further assumed to be strictly causal. The theory is trivially extended to the case where the perturbation, Δ, is block structured.

The mapping, $P_y : L_2[0, \infty) \to L_2[0, \infty)$, represents the nominal system, and $P_w : L_2(-\infty, \infty) \to L_2[0, \infty)$ models the effect of unknown (bounded) model noises and disturbances. The system $P_z : L_2[0, \infty) \to L_2[0, \infty)$ maps the system input to the perturbation and $P_v : L_2[0, \infty) \to L_2[0, \infty)$ maps the output of the perturbation to the system output.

We elect to use the notationally simpler assumption that all parts of the models are stable. The results consider a finite time experiment and we can relax the stability assumptions on P_z, P_v, and P_y, by considering the space of locally square integrable signals, L_2^{loc}, in place of L_2. Note that as

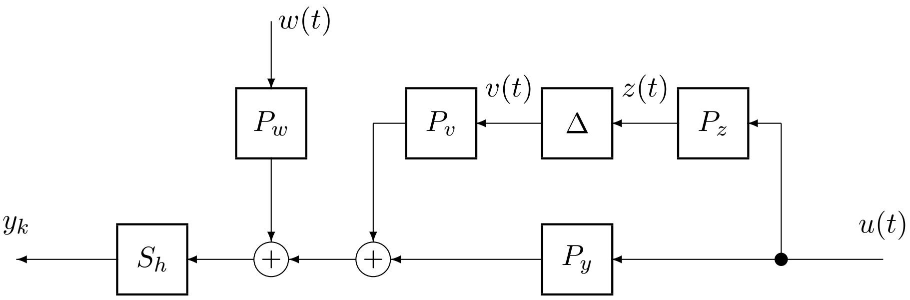

Figure 3: Block diagram of the system model for the validation problem

the disturbance, w, will be considered on an infinite horizon, we will always require P_w to be stable.

We will allow the noise and disturbance signals to be non-zero before the start of the experiment. That is, P_w maps $L_2(-\infty, \infty)$ to $L_2[0, \infty)$, and can therefore be partitioned as a map $[P_w^- \;\; P_w^+] : L_2(-\infty, 0) \oplus L_2[0, \infty) \to L_2[0, \infty)$. The mapping P_w^- captures the effect of signals having support on $(-\infty, 0)$ on the future interval $[0, \infty)$ and is given by

$$y(t) = C_w \int_{-\infty}^{0} e^{A_w(t-\tau)} B_w w(\tau)\, d\tau \tag{6}$$

where (A_w, B_w, C_w) is a stable realization of P_w. The map P_w^+ corresponds to the usual LTI system at rest at time zero.

The problem formulation assumes that $u(t)$ is known and therefore that $z(t)$ can be calculated. Typically, $u(t)$ might be formed by passing a computer generated discrete-time signal through a zero-order hold. No further assumptions are required on P_z or P_y, save that their outputs can be calculated from a knowledge of $u(t)$.

The assumptions on P_v and P_w are necessary to apply the framework that we will present. Knowledge of $z(t)$, using the calculation $z(t) = P_z u(t)$, gives a convex optimization problem.

The framework illustrated in Figure 3 applies to a significant number of typical robust control model configurations. One of the most commonly used is the multiplicative perturbation model illustrated in Figure 4. Additive perturbation models also fit the framework. What may not be clear, is that the approach we give also applies to models of closed-loop

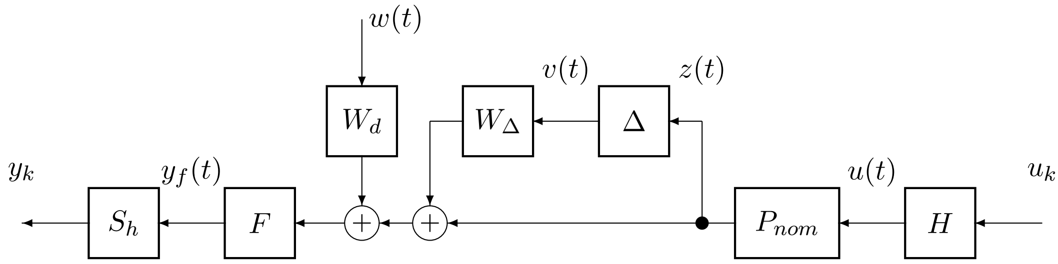

Figure 4: Model validation configuration for a multiplicative perturbation model with output disturbances

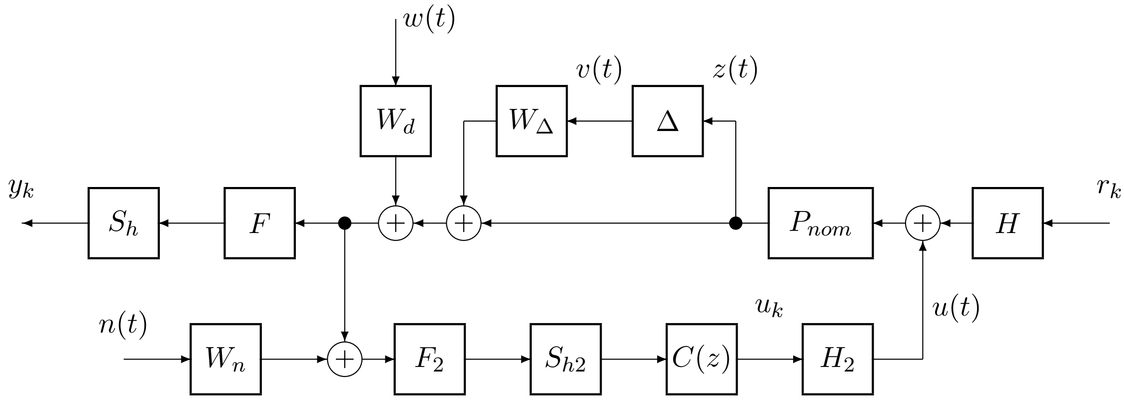

Figure 5: Model validation configuration for a closed-loop experiment

sampled-data systems, such as the one illustrated in Figure 5. For our approach to apply here we record the output of the controller, $C(z)$, and consider it as part of the datum.

Solution of the model validation problem involves finding the smallest norm w and Δ satisfying the equality constraint, (5). The next section develops the theoretical results required to characterize the existence of a perturbation Δ in terms of its input and output signals.

3.2 Extension Results for Perturbation Operators

This section contains results on extending operators in continuous-time. We start with two results, which are essentially corollaries of Propositions 1 and 2.

Proposition 3 *Suppose u and y are in $L_2[0,\infty)$, $T > 0$ and $h = \frac{T}{n+1}$ where n is a non-negative integer. Then there exists an h-anticipatory operator Δ on $L_2[0,\infty)$ satisfying,*

$$\Pi_T y = \Pi_T \Delta u, \qquad \textit{with } \|\Delta\| \leqslant 1, \tag{7}$$

if and only if,

$$\|\Pi_{kh} y\|_2 \leqslant \|\Pi_{kh} u\|_2 \qquad \textit{for } 1 \leqslant k \leqslant n+1. \tag{8}$$

Proof From the definition of Λ_h in (1) it is easy to see that

$$\Lambda_h \Pi^*_{(k+1)h} \Pi_{(k+1)h} = \pi^*_k \pi_k \Lambda_h,$$

where π_k is the truncation operator acting on $l_2(L_2[0,h))$. Now, given any operator Δ on $L_2[0,\infty)$, define $\tilde{\Delta} = \Lambda_h \Delta \Lambda_h^{-1}$; then clearly for each k

$$\Pi_{(k+1)h} \Delta \Pi^*_{(k+1)h} \Pi_{(k+1)h} = \Pi_{(k+1)h} \Delta \quad \text{if and only if} \quad \pi_k \tilde{\Delta} \pi^*_k \pi_k = \pi_k \tilde{\Delta}.$$

Therefore, the existence of a Δ as specified in the proposition is equivalent to the existence of a *causal* $\tilde{\Delta}$ on $l_2(L_2[0,h))$, with $\|\tilde{\Delta}\| \leqslant 1$, that satisfies

$$\tilde{y} = \pi_n \tilde{\Delta} \pi^*_n \tilde{u},$$

where $\tilde{y} = \pi_n \Lambda_h y$ and $\tilde{u} = \pi_n \Lambda_h u$. By Proposition 1 such a $\tilde{\Delta}$ exists if and only if $\sum_{k=0}^{l} \|\tilde{y}_k\|_2 \leqslant \sum_{k=0}^{l} \|\tilde{u}_k\|_2$ for $0 \leqslant l \leqslant n$. This latter condition is easily seen to be equivalent to (8); using the identity $\Lambda_h \Pi^*_{(k+1)h} \Pi_{(k+1)h} = \pi^*_k \pi_k \Lambda_h$. ■

The next proposition provides a result on the existence of periodic operators.

Proposition 4 *Suppose u and y are in $L_2[0,\infty)$, $T > 0$ and $h = \frac{T}{n+1}$ where n is a non-negative integer. Then there exists a both h-anticipatory and h-periodic operator Δ on $L_2[0,\infty)$ satisfying,*

$$\Pi_T y = \Pi_T \Delta u, \qquad \textit{with } \|\Delta\| \leqslant 1, \tag{9}$$

if and only if the matrix inequality,

$$\tilde{Y}_h^* \tilde{Y}_h \leqslant \tilde{U}_h^* \tilde{U}_h \qquad \textit{holds on } \mathcal{R}^{n+1}, \tag{10}$$

where $\tilde{Y}_h$ *and* $\tilde{U}_h$ *are defined as in (4) from the finite sequences* $\tilde{y} = \pi_n \Lambda_h y$ *and* $\tilde{u} = \pi_n \Lambda_h u$*.*

Proof To start observe from the definition of Λ_h in (1) that

$$\Lambda_h \Xi_h = \zeta \Lambda_h.$$

Therefore, an operator Δ on $L_2[0, \infty)$ is h-periodic if and only if $\tilde{\Delta} := \Lambda_h \Delta \Lambda_h^{-1}$ is *LTI* on $l_2(L_2[0, h))$.

Furthermore, from the proof of Proposition 3 we know Δ is h-anticipatory if and only if $\tilde{\Delta}$ is causal; and that the extension condition in (9) holds if and only if $\pi_n \tilde{y} = \pi_n \tilde{\Delta} \pi_n^* \tilde{u}$. By Proposition 2 such a $\tilde{\Delta}$ exists if and only if inequality (10) holds. ■

The next lemma is key in allowing us to apply the above results to obtain conditions for continuous-time causality and time-invariance.

Lemma 5 *Suppose the following three conditions hold:*

(i) The operator Δ *is the weak* limit of a uniformly bounded sequence* Δ_l *on* $L_2[0, \infty)$*.*

(ii) That $h_l > 0$ *is a strictly decreasing infinite sequence of real numbers tending to zero.*

(iii) The functions u *and* y *are elements of* $L_2[0, T)$*, where* $T > 0$*.*

Then

(a) If each Δ_l *satisfies* $\Pi_T \Delta_l \Pi_T^* u = y$*, then* $\Pi_T \Delta \Pi_T^* u = y$*.*

(b) If each Δ_l *is* h_l*-anticipatory, then* Δ *is causal.*

(c) If each Δ_l *is* h_l*-periodic, then* Δ *is LTI.*

Proof
<u>*Part a:*</u> Without loss of generality we assume $\|\Pi_T^* y\|_2 = 1$. By the weak* convergence we have

$$\langle \Pi_T^* \Pi_T \Delta \Pi_T^* u,\, \Delta_l \Pi_T^* u \rangle \xrightarrow{l \to \infty} \langle \Pi_T^* \Pi_T \Delta \Pi_T^* u,\, \Delta \Pi_T^* u \rangle = \|\Pi_T \Delta \Pi_T^* u\|_2^2,$$

and since $\Pi_T \Delta_l \Pi_T^* u = y$ obviously

$$\langle \Delta \Pi_T^* u,\, \Pi_T^* y \rangle = \|\Pi_T \Delta \Pi_T^* u\|_2^2.$$

Also, $\langle \Pi_T^* y, \Delta_l \Pi_T^* u \rangle \overset{l\to\infty}{\longrightarrow} \langle \Pi_T^* y, \Delta \Pi_T^* u \rangle$. Because the LHS=1, we conclude from the last equality that

$$1 = \langle \Pi_T^* y,\, \Delta \Pi_T^* u \rangle = \|\Pi_T \Delta \Pi_T^* u\|_2^2 = \|\Pi_T \Delta \Pi_T^* u\|_2\, \|\Pi_T^* y\|_2.$$

By the Cauchy-Schwartz inequality we immediately get

$$y = \Pi_T \Delta \Pi_T^* u.$$

<u>*Part b:*</u> We must show that

$$\Pi_t \Delta - \Pi_t \Delta \Pi_t^* \Pi_t = 0 \qquad \text{for all } t \geqslant 0. \tag{11}$$

It is sufficient to demonstrate that for every $u,\, x \in L_2[0,\infty)$ and $t_0 \in [0,\infty)$ we have

$$\langle \Pi_{t_0} x,\, (\Pi_{t_0} \Delta - \Pi_{t_0} \Delta \Pi_{t_0}^* \Pi_{t_0}) u \rangle = 0. \tag{12}$$

Choose and fix such u, x and t_0.

Next, let k_l be a positive sequence of integers so that $k_l h_l \overset{l\to\infty}{\longrightarrow} t_0$; this is always possible since h_l tends monotonically to zero. Hence, we see that

$$\Pi_{k_l h_l}^* \Pi_{k_l h_l} z \overset{l\to\infty}{\longrightarrow} \Pi_{t_0}^* \Pi_{t_0} z \qquad \text{for any } z \in L_2.$$

Using the last limit and the weak* convergence of Δ_l to Δ it follows that

$$\langle x,\, \Pi_{k_l h_l}^* \Pi_{k_l h_l} \Delta_l u \rangle \overset{l\to\infty}{\longrightarrow} \langle x,\, \Pi_{t_0}^* \Pi_{t_0} \Delta u \rangle$$

and

$$\langle x,\, \Pi_{k_l h_l}^* \Pi_{k_l h_l} \Delta_l \Pi_{k_l h_l}^* \Pi_{k_l h_l} u \rangle \overset{l\to\infty}{\longrightarrow} \langle x,\, \Pi_{t_0}^* \Pi_{t_0} \Delta \Pi_{t_0}^* \Pi_{t_0} u \rangle.$$

The latter two limits immediately imply that

$$\langle \Pi_{k_l h_l} x,\, (\Pi_{k_l h_l} \Delta_l - \Pi_{k_l h_l} \Delta_l \Pi_{k_l h_l}) u \rangle \overset{l\to\infty}{\longrightarrow} \langle \Pi_{t_0} x,\, (\Pi_{t_0} \Delta - \Pi_{t_0} \Delta \Pi_{t_0}^* \Pi_{t_0}) u \rangle.$$

Now, each Δ_l is h_l-causal; hence $\Pi_{k_l h_l} \Delta_l - \Pi_{k_l h_l} \Delta \Pi_{k_l h_l}^* \Pi_{k_l h_l} = 0$.
Therefore, by the last limit (11) holds since u, x and t_0 were arbitrary.

Part c: We will show that for all u, $x \in L_2$ and $t_0 > 0$, that

$$\langle x, (\Xi_{t_0}\Delta - \Delta\Xi_{t_0})u\rangle = 0. \tag{13}$$

Fix three such elements, and select a sequence k_l of positive integers so that $k_l h_l \overset{l\to\infty}{\longrightarrow} t_0$. Clearly, $\Xi_{k_l h_l} u \overset{l\to\infty}{\longrightarrow} \Xi_{t_0} u$ and $\Xi_{k_l h_l}\Delta u \overset{l\to\infty}{\longrightarrow} \Xi_{t_0}\Delta u$; see, e.g., [38, p. 134].

Because Δ is a weak* limit

$$\langle x, \Xi_{t_0}\Delta_l u\rangle \overset{l\to\infty}{\longrightarrow} \langle x, \Xi_{t_0}\Delta u\rangle \quad \text{and} \quad \langle x, \Delta_l \Xi_{t_0} u\rangle \overset{l\to\infty}{\longrightarrow} \langle x, \Delta\Xi_{t_0} u\rangle.$$

From this and the former two limits we immediately arrive at

$$\langle x, \Xi_{k_l h_l}\Delta_l u\rangle \overset{l\to\infty}{\longrightarrow} \langle x, \Xi_{t_0}\Delta u\rangle \quad \text{and} \quad \langle x, \Delta_l \Xi_{k_l h_l} u\rangle \overset{l\to\infty}{\longrightarrow} \langle x, \Delta\Xi_{t_0} u\rangle.$$

We know for each l that $\Xi_{k_l h_l}\Delta_l - \Delta_l \Xi_{k_l h_l} = 0$. Therefore, adding the last two limits, and noting t_0, x and u were arbitrary we have (13). ∎

The next two results give extension conditions for causal and LTI perturbations. Although they are not explicitly used in the sequel we present them because of their relevance to the continuous time model validation problem. We can now prove the following theorem, which is the continuous-time analogue of Proposition 3.

Theorem 6 *Suppose z, $v \in L_2[0, T)$, where $T > 0$. Then there exists a causal operator, Δ, on $L_2[0, \infty)$ satisfying,*

$$v = \Pi_T \Delta \Pi_T^* z, \quad \textit{with } \|\Delta\| \leqslant 1,$$

if and only if,

$$\|\Pi_t \Pi_T^* v\|_2 \leqslant \|\Pi_t \Pi_T^* z\|_2 \quad \textit{for all } t \in [0, T].$$

Proof (only if): Suppose the inequality is violated, then for some t_0

$$\|\Pi_{t_0}\Pi_T^* v\|_2 > \|\Pi_{t_0}\Pi_T^* z\|_2.$$

Therefore, if there exists a Δ satisfying $v = \Pi_T \Delta \Pi_T^* z$ we have

$$\|\Pi_{t_0}\Delta\Pi_T^* z\|_2 = \|\Pi_{t_0}\Pi_T^* v\|_2 > \|\Pi_{t_0}\|\,\|\Delta\|\,\|\Pi_{t_0}^*\Pi_{t_0}\Pi_T^* z\|_2 \geqslant \|\Pi_{t_0}\Delta\Pi_{t_0}^*\Pi_{t_0}\Pi_T^* z\|_2.$$

So, Δ is not causal; this completes the contrapositive argument.

(if): Start by choosing a sequence $h_l > 0$ that tends monotonically to zero, such that T/h_l is an integer for every l. Now, by the hypothesis for each l we have

$$\|\Pi_{h_l k}\Pi_T^* v\|_2 \leqslant \|\Pi_{h_l k}\Pi_T^* z\|_2 \qquad \text{for all } 0 \leqslant k \leqslant (\tfrac{T}{h_l}).$$

Invoking Proposition 3 we have that there exists a sequence operators Δ_l, with $\|\Delta_l\| \leqslant 1$, each being h_l-causal, that satisfy

$$\Pi_T \Delta_l \Pi_T^* z = v.$$

Since the sequence Δ_l is bounded by one, we may assume without loss of generality that it converges weak* to some operator Δ; clearly $\|\Delta\| \leqslant 1$. By Lemma 5 (a) we have that $\Pi_T \Delta \Pi_T^* z = v$ is satisfied; Part (b) guarantees Δ is causal. ■

To state the next set of results we require a new operator: given z in $L_2^m[0,T)$, where $T > 0$, define the integral operator $Z : L_2^1[0,\,T) \to L_2^m[0,\,T)$ via the integral kernel

$$Z(t,\,\tau) := \begin{cases} z(t-\tau) & 0 \leqslant t-\tau \leqslant T \\ 0 & \text{otherwise.} \end{cases}$$

Then the operator Z is defined by

$$(Zw)(t) := \int_0^T Z(t,\tau)w(\tau)\,d\tau \tag{14}$$

We remark that such an operator has an adjoint which we denote by Z^*. The following result is a continuous time analogue to Proposition 4.

Theorem 7 *Suppose $z,\, v \in L_2[0,T)$, where $T > 0$. Then there exists an LTI, causal, operator, Δ, satisfying,*

$$v = \Pi_T \Delta \Pi_T^* z, \quad \textit{with } \|\Delta\| \leqslant 1,$$

if and only if the operator inequality

$$V^*V \leqslant Z^*Z \quad \textit{holds,}$$

where V and Z are operators on $L_2[0,T)$ defined, as in (14), from v and z respectively.

The proof of this theorem requires the following technical lemma.

Lemma 8 *Suppose z, $v \in L_2[0,T)$, where $T > 0$. Define the operators Z and V, from z and v as in (14), and, given $h > 0$, define $\tilde{Z}_h$ and $\tilde{V}_h$ from $\tilde{v} = \Lambda_h v$ and $\tilde{u} = \Lambda_h u$ as in (4). Then*

(i) If $V^*V \leqslant Z^*Z$, then for each integer $n > 0$ the inequality $\tilde{V}_h^*\tilde{V}_h \leqslant \tilde{Z}_h^*\tilde{Z}_h$ holds, where $h := T/n$.

(ii) If the matrix inequalities $\tilde{V}_h^*\tilde{V}_h \leqslant \tilde{Z}_h^*\tilde{Z}_h$ hold for all integers $n > 0$, with $h = T/n$, then the operator inequality $V^*V \leqslant Z^*Z$ is satisfied.

The proof of this lemma can be found in Appendix A.

Proof of Theorem 7
(only if): If such a Δ exists, it is clearly both h-anticipatory and h-periodic for all $h > 0$. Therefore, by Proposition 4 the inequality $\tilde{V}_h^*\tilde{V}_h \leqslant \tilde{Z}_h^*\tilde{Z}_h$ holds for all $h > 0$. Now, invoke Lemma 8 (ii) to conclude that $V^*V \leqslant Z^*Z$.

(if): Begin by defining the sequence $h_l := T/l$. Because $V^*V \leqslant Z^*Z$, Lemma 8 Part (i) guarantees that $\tilde{V}_{h_l}^*\tilde{V}_{h_l} \leqslant \tilde{Z}_{h_l}^*\tilde{Z}_{h_l}$ for all l. Hence, by Proposition 4 we have that there exists a sequence Δ_l of operators, each being both h_l-periodic and h_l-anticipatory, satisfying $v = \Pi_T\Delta_l\Pi_T^* z$ with $\|\Delta_l\| = 1$.

Since the sequence Δ_l is uniformly bounded, we assume without loss of generality that it converges weak* to an operator Δ. By Lemma 5 the operator Δ has the desired properties. ■

3.3 Model Validation Results

In this section we develop and present necessary and sufficient conditions for an experimental datum to invalidate the model arrangement of Figure 3. The conditions constructed can be evaluated as convex programs, and the details of this are presented in Section 4.

Recall that h is the sampling period of S_h, and is assumed to be fixed throughout. A key step to determining whether this model can produce the observations y_k is determining the set of signals that could have produced y_k. In the next subsection we consider this problem.

3.3.1 Solution Framework

This subsection is devoted to examining the structure of the operators P_v and P_w, and solving a particular type of equation associated with the model of Figure 3.

We start by considering an alternative, and convenient, representation for $S_h P_v$. Since $S_h P_v$ maps $L_2[0,\infty)$ to $l_2(\mathcal{R}^m)$, it has a representation as a mapping from $l_2(L_2[0,h)\,)$ to $l_2(\mathcal{R}^m)$, which can be defined by $\tilde{P}_v := S_h P_v \Lambda_h^{-1}$. Specifically, given a realization $(A_v,\, B_v,\, C_v)$ for the strictly causal system P_v, the relationship $y = \tilde{P}_v \tilde{v}$ can be realized by the equations

$$\begin{aligned} x_{k+1} &= \tilde{A}_v x_k + \tilde{B}_v \tilde{v}_k, \qquad x_0 = 0, \\ y_k &= C_v x_k, \end{aligned} \tag{15}$$

where $\tilde{A}_v = e^{A_v h}$ is an $a_v \times a_v$ matrix, and $\tilde{B}_v : L_2[0,h) \to \mathcal{R}^{a_v}$ is an operator defined by

$$\tilde{B}_v \tilde{v}_k = \int_0^h e^{A_v(h-\tau)} B_v \tilde{v}_k(\tau)\, d\tau.$$

This representation for $\tilde{P}_v$ is easily found by considering the evolution of P_v over each time interval $[kh,\, (k+1)h)$. See [28] and Appendix B for a detailed development.

We now state the main problem considered in this subsection: Given an integer $n > 0$ and a sequence $q \in \{0\} \oplus \left(\bigoplus_{k=1}^{n} \mathcal{R}^m \right)$, find all solutions $v \in L_2[0,\infty)$ such that

$$q = \pi_n S_h P_v v.$$

Observe that, since P_v is strictly causal, the first entry in q must be equal to zero. Our approach to solving this function equation is by considering a similar equation using the lifted system $\tilde{P}_v$.

Lemma 9 *Suppose $q \in \{0\} \oplus \left(\bigoplus_{k=1}^{n} \mathcal{R}^m \right)$, where $n \geqslant 1$, and $v \in L_2[0,\infty)$. Then $q = \pi_n S_h P_v v$ if and only if*

$$q = \pi_n \tilde{P}_v \pi_{n-1}^* \tilde{v} \quad \textit{where} \quad \tilde{v} = \pi_{n-1} \Lambda_h v. \tag{16}$$

We use the following fact in the proof of the above lemma:

Lemma 10 *If $n \geqslant 1$ is an integer, then $\pi_n S_h P_v = \pi_n S_h P_v \Pi_{nh}^* \Pi_{nh}$.*

The preceding lemma can be easily proved from the definitions of π_n and Π_{nh}, and the fact P_v is LTI and causal.

Proof of Lemma 9 (only if): From Lemma 10 we can substitute to get

$$q = \pi_n S_h P_v v = \pi_n S_h P_v \Pi_{nh}^* \Pi_{nh} v = \pi_n S_h P_v \Pi_{nh}^* \Pi_{nh} \Lambda_h^{-1} \Lambda_h v.$$

Using the property $\Pi_{nh}^* \Pi_{nh} \Lambda_h^{-1} = \Lambda_h^{-1} \pi_{n-1}^* \pi_{n-1}$ the above yields

$$q = \pi_n S_h P_v \Lambda_h^{-1} \pi_{n-1}^* \pi_{n-1} \Lambda_h v = \pi_n \tilde{P}_v \pi_{n-1}^* \tilde{v}.$$

(if): This part follows by reversing the above argument. ■

From the definition of π_n and the representation of $\tilde{P}_v$ in (15) it is easy that $\tilde{v}$ is a solution to (16) if and only if

$$\begin{bmatrix} q_1 \\ q_2 \\ \vdots \\ q_n \end{bmatrix} = \begin{bmatrix} C_v \tilde{B}_v & 0 & \cdots & 0 \\ C_v \tilde{A}_v \tilde{B}_v & \ddots & & 0 \\ \vdots & \ddots & & \vdots \\ C_v \tilde{A}_v^{n-1} \tilde{B}_v & \cdots & C_v \tilde{A}_v \tilde{B}_v & C_v \tilde{B}_v \end{bmatrix} \begin{bmatrix} \tilde{v}_0 \\ \tilde{v}_1 \\ \vdots \\ \tilde{v}_{n-1} \end{bmatrix}. \quad (17)$$

Hence to parametrize all solutions to (16) it is sufficient to find all solutions to (17).

We accomplish this by examining the action of the operator $\tilde{B}_v$. First, let $\mathcal{N}(\tilde{B}_v)$ denote the kernel of $\tilde{B}_v$; since it is a closed subspace of $L_2[0,h)$ it has an orthogonal complement $\mathcal{N}^{\perp}(\tilde{B}_v)$ so that

$$L_2[0,h) = \mathcal{N}(\tilde{B}_v) \oplus \mathcal{N}^{\perp}(\tilde{B}_v).$$

Hence, all solutions $\tilde{v} = (\tilde{v}_0, \ldots, \tilde{v}_{n-1}) \in \bigoplus_{k=0}^{n-1} L_2[0,h)$ to (17) can be decomposed into two parts

$$\tilde{v} = \tilde{v}^{\dagger} + \tilde{v}^{\ddagger} \quad (18)$$

where for each $0 \leqslant k \leqslant n-1$, we have $\tilde{v}_k^{\dagger} \in \mathcal{N}^{\perp}(\tilde{B}_v)$ and $\tilde{v}_k^{\ddagger} \in \mathcal{N}(\tilde{B}_v)$, and $\tilde{v}^{\dagger}$ satisfies (17).

Now, it is well-known that the dimension of the image of an operator is equal to the co-dimension of the kernel of the operator. So,

$$\dim(\mathcal{N}^{\perp}(\tilde{B}_v)) = \dim(\mathrm{Im}(\tilde{B}_v)) =: b_v$$

which is necessarily finite since $\mathrm{Im}(\tilde{B}_v) \subset \mathcal{R}^{a_v}$. Because $\mathcal{N}^\perp(\tilde{B}_v)$ is a finite dimensional subspace of a Hilbert space, it is isometrically isomorphic to $\mathcal{R}^{b_v}$. Namely, there exists a map $U_v : \mathcal{R}^{b_v} \to \mathcal{N}^\perp(\tilde{B}_v)$ so that $\mathrm{Im}(U_v) = \mathcal{N}^\perp(\tilde{B}_v)$ and

$$\langle U_v x, U_v y\rangle = \langle x, y\rangle \quad \text{for all } x, y \in \mathcal{R}^{b_v}.$$

At the moment we do not require an explicit representation for such a U_v; but one is provided in Appendix B. For convenience define the matrix

$$\bar{B}_v := \tilde{B}_v U_v \tag{19}$$

and the diagonal operator $\tilde{U}_v$ mapping $\bigoplus_{k=0}^{n-1} \mathcal{R}^{b_v}$ to $\bigoplus_{k=0}^{n-1} L_2[0,h)$ by

$$\tilde{U}_v := \mathrm{diag}(U_v, \ldots, U_v). \tag{20}$$

Making use of the definitions so far, we have the following result.

Proposition 11 *All solutions* $\tilde{v} = (\tilde{v}_0, \ldots, \tilde{v}_{n-1}) \in \bigoplus_{k=0}^{n-1} L_2[0,h)$ *to (17) are given by*

$$\tilde{v} = \tilde{U}_v \bar{v} + \tilde{v}^\ddagger,$$

where $\tilde{v}^\ddagger \in \bigoplus_{k=0}^{n-1} \mathcal{N}(\tilde{B}_v)$ *and* $\bar{v}$ *is a vector in* $\bigoplus_{k=0}^{n-1} \mathcal{R}^{b_v}$ *that satisfies*

$$(q_1, \ldots, q_n) = \bar{P}_v \bar{v}, \tag{21}$$

where

$$\bar{P}_v := \begin{bmatrix} C_v\bar{B}_v & 0 & \cdots & 0 \\ C_v\tilde{A}_v\bar{B}_v & \ddots & & 0 \\ \vdots & \ddots & & \vdots \\ C_v\tilde{A}_v^{n-1}\bar{B}_v & \cdots & C_v\tilde{A}_v\bar{B}_v & C_v\bar{B}_v \end{bmatrix}. \tag{22}$$

Proof Suppose that $\tilde{v}$ is a solution to (17). Then from the definitions leading up to (18) we know that it can be decomposed as $\tilde{v} = \tilde{v}^\dagger + \tilde{v}^\ddagger$ where $\tilde{v}_k^\dagger \in \mathcal{N}^\perp(\tilde{B}_v)$ and $\tilde{v}_k^\ddagger \in \mathcal{N}(\tilde{B}_v)$ for each $0 \leqslant k \leqslant n-1$.

Since $\mathrm{Im}(U_v)$=$\mathcal{N}^\perp(\tilde{B}_v)$ there exist vectors $\bar{v}_k \in \mathcal{R}^{b_v}$ so that $U_v\bar{v}_k = \tilde{v}_k^\dagger$, or equivalently, $\tilde{v}^\dagger = \tilde{U}_v\bar{v}$.

To see that (21) holds, note that $\tilde{v}^\dagger$ satisfies (17); therefore the substitution $\tilde{v}^\dagger = (U_v\bar{v}_0, \ldots, U_v\bar{v}_{n-1})$ yields (21) using the definition of $\bar{B}_v$.

Reversing the argument, it is routine to verify that any $\tilde{v} = \tilde{U}_v \bar{v} + \tilde{v}^{\ddagger}$ satisfies (17). ■

Our next step is to examine a similar equation associated with the operator P_w. Recall that P_w maps $L_2(-\infty, \infty)$ to $L_2[0, \infty)$, and can be decomposed into the Hankel operator P_w^- realized in (6), and the LTI system at rest, $P_w^+ : L_2[0, \infty) \to L_2[0, \infty)$. We define an associated lifted system $\tilde{P}_w$ mapping $L_2(-\infty, 0) \oplus l_2(L_2[0, h))$ to $l_2(\mathcal{R}^m)$, by $\tilde{P}_w := S_h[P_w^- \;\; P_w^+ \Lambda_h^{-1}]$, which is analogous to $\tilde{P}_v$ above. The map $S_h P_w^+ \Lambda_h^{-1}$ has a realization of the form in (15). Thus, using (6) we can realize $y = \tilde{P}_w \begin{bmatrix} \tilde{w}^- \\ \tilde{w}^+ \end{bmatrix}$ by the difference equations,

$$\begin{aligned} x_{k+1} &= \tilde{A}_w x_k + \tilde{B}_w^+ \tilde{w}_k^+, \qquad x_0 = \tilde{B}_w^- \tilde{w}^- \\ y_k &= C_w x_k \end{aligned} \tag{23}$$

where the matrix $\tilde{A}_w = e^{A_w h}$ has dimension $a_w \times a_w$, and $\tilde{B}_w^+ : L_2[0, h) \to \mathcal{R}^{a_w}$ and $\tilde{B}_w^- : L_2(-\infty, 0) \to \mathcal{R}^{a_w}$ and are defined by

$$\tilde{B}_w^+ \tilde{w}_k^+ = \int_0^h e^{A_w(h-\tau)} B_w \tilde{w}_k^+(\tau)\, d\tau, \qquad \tilde{B}_w^- \tilde{w}^- = \int_{-\infty}^0 e^{-A_w(\tau)} B_w \tilde{w}^-(\tau)\, d\tau. \tag{24}$$

Similar to the preceding analysis on $\tilde{P}_v$, here we aim to characterize all solutions $w \in L_2(-\infty, \infty)$ that satisfy $q = \pi_n S_h P_w w$:

Lemma 12 *Suppose $q \in \bigoplus_{k=0}^{n} \mathcal{R}^{c_v}$, where $n \geqslant 0$, and $w = (w^-, w^+) \in L_2(-\infty, 0) \oplus L_2[0, \infty)$. Then $q = \pi_n S_h P_w w$ if and only if*

$$q = \pi_n \tilde{P}_w \pi_n^* \tilde{w}, \tag{25}$$

where $\tilde{w} = (w^-, \tilde{w}_0^+, \tilde{w}_1^+, \ldots, \tilde{w}_{n-1}^+)$ and $\tilde{w}^+ = \pi_{n-1} \Lambda_h w^+$.

Since the proof is largely the same as that of Lemma 9, and therefore it is not included. Note however that here, unlike in (16), q is not constrained to have zero as its first entry; this is because w can have support on the entire interval $(-\infty, \infty)$.

As with (17), $(\tilde{w}^-, \tilde{w}^+)$ is a solution to (25) if and only if

$$\begin{bmatrix} q_0 \\ q_1 \\ \vdots \\ q_{n-1} \\ q_n \end{bmatrix} = \begin{bmatrix} C_w\tilde{B}_w^- & 0 & & \cdots & 0 \\ C_w\tilde{A}_w\tilde{B}_w^- & C_w\tilde{B}_w^+ & 0 & \cdots & 0 \\ \vdots & C_w\tilde{A}_w\tilde{B}_w^+ & \ddots & & 0 \\ & \vdots & \ddots & & \vdots \\ C_w\tilde{A}_w^n\tilde{B}_w^- & C_w\tilde{A}_w^{n-1}\tilde{B}_w^+ & \cdots & C_w\tilde{A}_w\tilde{B}_w^+ & C_w\tilde{B}_w^+ \end{bmatrix} \begin{bmatrix} \tilde{w}^- \\ \tilde{w}_0^+ \\ \tilde{w}_1^+ \\ \vdots \\ \tilde{w}_{n-1}^+ \end{bmatrix}. \tag{26}$$

Observe that $\tilde{B}_w^-$ and $\tilde{B}_w^+$ are both finite rank operators; in fact using (24) and a state space reachability argument, it is routine to show that these operators have equal rank. We therefore employ the same reasoning used above to define U_w, to obtain the existence of isometries $U_w^- : \mathcal{R}^{b_w} \to \mathcal{N}^\perp(\tilde{B}_w^-)$ and $U_w^- : \mathcal{R}^{b_w} \to \mathcal{N}^\perp(\tilde{B}_w^+)$. With these define further,

$$\begin{aligned} \bar{B}_w^- &:= \tilde{B}_w^- U_w^-, \\ \bar{B}_w^+ &:= \tilde{B}_w^+ U_w^+, \\ \tilde{U}_w &:= \operatorname{diag}(U_w^-, U_w^+, \ldots, U_w^+). \end{aligned}$$

Using these definitions we have the following result.

Proposition 13 *All solutions* $\tilde{w} = (\tilde{w}^-, \tilde{w}_0^+, \ldots, \tilde{w}_{n-1}^+) \in L_2(-\infty, 0) \oplus \left(\bigoplus_{k=0}^{n-1} L_2[0, h] \right)$ *to (26) are given by*

$$\tilde{w} = \tilde{U}_w \bar{w} + \tilde{w}^\ddagger,$$

where $\tilde{w}^\ddagger \in \mathcal{N}(\tilde{B}_w^-) \oplus \left(\bigoplus_{k=0}^{n-1} \mathcal{N}(\tilde{B}_w^+) \right)$ *and* $\bar{w}$ *is a vector in* $\bigoplus_{k=0}^{n} \mathcal{R}^{b_w}$ *that satisfies*

$$q = \bar{P}_w \bar{w}, \tag{27}$$

where

$$\bar{P}_w := \begin{bmatrix} C_w\bar{B}_w^- & 0 & & \cdots & 0 \\ C_w\tilde{A}_w\bar{B}_w^- & C_w\bar{B}_w^+ & 0 & \cdots & 0 \\ \vdots & C_w\tilde{A}_w\bar{B}_w^+ & \ddots & & 0 \\ & \vdots & \ddots & & \vdots \\ C_w\tilde{A}_w^n\bar{B}_w^- & C_w\tilde{A}_w^{n-1}\bar{B}_w^+ & \cdots & C_w\tilde{A}_w\bar{B}_w^+ & C_w\bar{B}_w^+ \end{bmatrix}. \tag{28}$$

Since this proof is not significantly different from that of Proposition 11 it is omitted.

3.3.2 Invalidation Conditions: Basic Case

We now apply the result of the last section to deriving conditions which answer the model validation question posed in Section 2.4. Our results provide conditions, given an input u and an finite observed sequence y_k, under which there exists an appropriate perturbation Δ and noise signal w that make Figure 3 consistent with the observed datum $(y_k, u(t))$. For convenience in stating our model validation results we have the following formal definition.

Definition 14 *Given* $u \in L_2[0,\infty)$ *and* $y \in \bigoplus_{k=0}^{n} \mathcal{R}^{c_v}$. *The model in Figure 3 is* not invalidated *with respect to the perturbation set* $\mathcal{X}$ *if there exists a perturbation* $\Delta \in \mathcal{X}$, *with* $\|\Delta\|_{L_2 \to L_2} \leqslant 1$ *and a signal* $w \in BL_2(-\infty,\infty)$, *such that*

$$y = \pi_n S_h(P_w w + (P_v \Delta P_z + P_y)u).$$

We now prove the first model validation result; the theorem statement uses the matrices $\bar{P}_v$ and $\bar{P}_w$ defined in Propositions 11 and 13.

Theorem 15 *Suppose* $u \in L_2[0,\infty)$, $y \in \bigoplus_{k=0}^{n} \mathcal{R}^{c_v}$, *and define* $z = P_z u$. *Then the model in Figure 3 is* not invalidated *with respect to* h*-anticipatory perturbations if and only if there exist vectors* $\bar{v} \in \bigoplus_{k=0}^{n-1} \mathcal{R}^{b_v}$ *and* $\bar{w} \in \bigoplus_{k=0}^{n} \mathcal{R}^{b_w}$, *with* $|\bar{w}|_2 \leqslant 1$, *satisfying*

$$y - \pi_n S_h P_y u = [\bar{P}_v \quad \bar{P}_w] \begin{bmatrix} \bar{v} \\ \bar{w} \end{bmatrix}$$

and

$$\sum_{k=0}^{l-1} |\bar{v}_k|_2^2 \leqslant \|\Pi_{lh} z\|_2 \quad \text{for } 1 \leqslant l \leqslant n+1. \tag{29}$$

Proof (only if): Suppose that Δ and w satisfy the hypothesis. Define

$$v := \Delta P_z u.$$

Since Δ is h-anticipatory we have that

$$\|\Pi_{lh} v\|_2 \leqslant \|\Pi_{lh} z\|_2 \qquad \text{for all } 1 \leqslant l \leqslant n+1. \tag{30}$$

Also by assumption the following equation holds:

$$y - \pi_n S_h P_y u = \pi_n S_h [P_w \;\; P_v] \begin{bmatrix} w \\ v \end{bmatrix}. \tag{31}$$

Applying Lemmas 9 and 12 the above implies

$$y - \pi_n S_h P_y u = \pi_n [\tilde{P}_w \;\; \tilde{P}_v] \begin{bmatrix} \pi_n^* \tilde{w} \\ \pi_{n-1}^* \tilde{v} \end{bmatrix}.$$

Now, invoking Propositions 11 and 13 we can decompose $\tilde{w} = \tilde{U}_w \bar{w} + \tilde{w}^\ddagger$ and $\tilde{v} = \tilde{U}_v \bar{v} + \tilde{v}^\ddagger$ to get

$$y - \pi_n S_h P_y u = \pi_n [\tilde{P}_w \;\; \tilde{P}_v] \begin{bmatrix} \pi_n^* (\tilde{U}_w \bar{w} + \tilde{w}^\ddagger) \\ \pi_{n-1}^* (\tilde{U}_v \bar{v} + \tilde{v}^\ddagger) \end{bmatrix} = [\bar{P}_w \;\; \bar{P}_v] \begin{bmatrix} \bar{w} \\ \bar{v} \end{bmatrix}.$$

So, to complete the proof we must show that $\bar{v}$ and $\bar{w}$ satisfy the norm constraints. Using the orthogonality properties of the above decomposition,

$$\|\tilde{w}\|_2 = \sum_{k=0}^{n} |\bar{w}_k|_2^2 + \sum_{k=0}^{n} \|\tilde{w}_k^\ddagger\|_2^2 \quad \text{and} \quad \|\tilde{v}\|_2 = \sum_{k=0}^{n-1} |\bar{v}_k|_2^2 + \sum_{k=0}^{n-1} \|\tilde{v}_k^\ddagger\|_2^2.$$

Therefore the required norm conditions follow using the assumption $\|w\|_2 \leqslant 1$ and (30).

(if): Start by setting $\tilde{v} = \tilde{U}_v \bar{v}$ and $\tilde{w} = \tilde{U}_w \bar{w}$, and reversing the above argument to get (31) and (30). The norm condition required on w is clearly met.

Now using $\pi_n S_h P_v = \pi_n S_h P_v \Pi_{nh}^* \Pi_{nh}$, from Lemma 10, in (31) yields

$$y - \pi_n S_h P_y u = \pi_n S_h [P_w \;\; P_v] \begin{bmatrix} w \\ \Pi_{nh}^* \Pi_{nh} v \end{bmatrix}. \tag{32}$$

Also, from (30) and Proposition 3 there exists an h-anticipatory operator, Δ, such that $\|\Delta\|_{L_2 \to L_2} \leqslant 1$ and

$$\Pi_{nh}^* \Pi_{nh} v = \Pi_{nh}^* \Pi_{nh} \Delta \Pi_{nh}^* \Pi_{nh} z = \Pi_{nh}^* \Pi_{nh} \Delta z.$$

Substituting this into (32), and again using Lemma 10, we get

$$y - \pi_n S_h P_y u = \pi_n S_h [P_w \;\; P_v] \begin{bmatrix} w \\ \Delta z \end{bmatrix}, \tag{33}$$

and so the model is not invalidated. ■

The above result provides exact conditions for invalidation with respect to h-anticipatory perturbations. The next theorem is its counterpart which further limits the perturbations to be h-periodic.

Theorem 16 *Suppose* $u \in L_2[0,\infty)$, $y \in \bigoplus_{k=0}^{n} \mathcal{R}^{c_v}$, *and define* $z = P_z u$ *and* $\tilde{z} = \pi_{n-1}\Lambda_h z$. *Then the model in Figure 3 is* not invalidated *with respect to h-anticipatory, h-periodic, perturbations if and only if there exist vectors* $\bar{v} \in \bigoplus_{k=0}^{n-1} \mathcal{R}^{b_v}$ *and* $\bar{w} \in \bigoplus_{k=0}^{n} \mathcal{R}^{b_w}$, *with* $|\bar{w}|_2 \leqslant 1$, *such that*

$$y - \pi_n S_h P_y u = [\bar{P}_v \quad \bar{P}_w]\begin{bmatrix} \bar{v} \\ \bar{w} \end{bmatrix}$$

and

$$\bar{V}^*\bar{V} \leqslant \tilde{Z}_h^*\tilde{Z}_h, \tag{34}$$

where $\bar{V}$ *and* $\tilde{Z}_h$ *are defined from* $\bar{v}$ *and* $\tilde{z}$ *respectively, as in (4).*

Proof (only if): Suppose that Δ and w satisfy the hypothesis: set $v = \Delta P_z z$, and by Proposition 4 we have

$$\tilde{V}_h^*\tilde{V}_h \leqslant \tilde{Z}_h^*\tilde{Z}_h,$$

where $\tilde{V}_h$ is defined by $\tilde{v} = \pi_{n-1}\Lambda_h v$ and (4). From Proposition 11 we can decompose $\tilde{v} = \tilde{U}_v\bar{v} + \tilde{v}^\ddagger$. The orthogonality of $U_v\bar{v}_k$ and $\tilde{v}_l^\ddagger$ for every k and l gives,

$$\tilde{V}_h^*\tilde{V}_h = \bar{V}^*\bar{V} + (\tilde{V}_h^\ddagger)^*\tilde{V}_h^\ddagger,$$

where $\bar{V}$ and $\tilde{V}_h^\ddagger$ are defined from $\bar{v}$ and $\tilde{v}^\ddagger$ as in (4). Hence, $\bar{V}^*\bar{V} \leqslant \tilde{Z}_h^*\tilde{Z}_h$. The other properties of $\bar{v}$ and $\bar{w}$ are proved exactly as in Theorem 15.

(if): Set $\tilde{v} = \tilde{U}_v\bar{v}$ and $\tilde{w} = (\tilde{w}^-, \tilde{w}_0^+, \ldots, \tilde{w}_{n-1}^+) = \tilde{U}_w\bar{w}$, and note that

$$\tilde{V}_h^*\tilde{V}_h = \bar{V}^*\bar{V} \leqslant \tilde{Z}_h^*\tilde{Z}_h.$$

With $v = \Lambda_h^{-1}\pi_n^*\tilde{v}$ we invoke Proposition 4 to get that there exists an h-anticipatory and h-periodic operator, Δ, satisfying

$$\Pi_{nh}v = \Pi_{nh}\Delta z.$$

We then define $w = (\tilde{w}^-, \Lambda_h^{-1}\pi_{n-1}^*\tilde{w}^+) \in L_2(-\infty,0) \oplus L_2[0,\infty)$ and follow the same steps as in the 'if' part of Theorem 15 to get (33). ■

3.3.3 Invalidation Conditions: General Case

In the preceding subsection exact conditions for invalidation with respect to h-periodic and h-anticipatory perturbations were constructed, where h

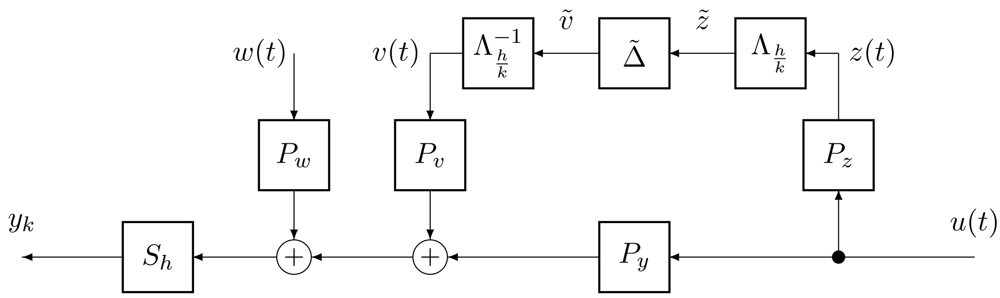

Figure 6: Framework for applying fast lifting operators to the perturbation

is the sampling interval of our data. While these results may be useful in many model validation scenarios, we now derive conditions for invalidation where the periodicity and degree of approximation to causality can be further specified. Namely, we extend the results of the last section so that we can invalidate a model, given observations y, to $\frac{h}{k}$-periodic and $\frac{h}{k}$-anticipatory perturbations, where $\frac{h}{k}$ can be chosen as small as desired by choosing the integer $k > 0$ to be large.

The procedure is illustrated conceptually in Figure 6. The lifting and inverse lifting operators are considered over an integer fraction of the sample time interval. By making $\frac{h}{k}$ smaller, the $\frac{h}{k}$-periodicity and $\frac{h}{k}$-anticipatory perturbation results approximate linear time-invariance and causality as closely as desired. This approach does not require additional experimental data as the formulation preserves the sampling period, h, on the output of P_v. However, the dimension of the characterization of the perturbation (as given in (29) and (34)), increases. The following details this approach.

To derive the conditions in Theorems 15 and 16 we used the structure of the solutions to (16) given in Proposition 11. The key was to separate the solutions, as in (18), into two components, one from a finite dimensional subspace and the other from an infinite dimensional one. We then found when proving the invalidation results that it was sufficient to consider solutions solely in the finite dimensional subspace. We now perform a similar decomposition on the equation,

$$y = \pi_n S_h P_v \Lambda^{-1}_{\frac{h}{k}} \pi^*_{nk-1} \tilde{v}, \tag{35}$$

where $\tilde{v} \in \bigoplus_{l=0}^{nk-1} L_2[0, \frac{h}{k})$.

To start, it is convenient to introduce a decimation operator, $\Gamma_k : l_2 \to l_2$, by defining, for each integer $k > 0$,

$$(\Gamma_k\, y\,)_l = y(kl) \quad \text{for each integer } l \geqslant 0,$$

where $y \in l_2$. In words, it is the mapping that selects every kth member of the sequence. Using this definition it is routine to verify that

$$\Gamma_k S_{\frac{h}{k}} = S_h \quad \text{and} \quad \pi_n \Gamma_k \pi^*_{kn} \pi_{kn} = \pi_n \Gamma_k, \tag{36}$$

for all integers $n \geqslant 0$, $k > 0$.

To state the next result we require some new definitions: define the matrices and operator,

$$\begin{aligned} \tilde{A}^{(k)}_v &:= e^{\tilde{A}_v \frac{h}{k}}, \\ \bar{B}^{(k)}_v &:= \tilde{B}^{(k)}_v U^{(k)}_v, \\ \tilde{U}^{(k)}_v &:= \operatorname{diag}(U^{(k)}_v, \ldots, U^{(k)}_v), \end{aligned}$$

where $\tilde{B}^{(k)}_v \psi := \int_0^{\frac{h}{k}} e^{A_v(\frac{h}{k} - \tau)} B_v \psi(\tau)\, d\tau$ and $U^{(k)}_v$ is any fixed isometry mapping $\mathcal{R}^{b_v}$ to $\mathcal{N}^{\perp}(\tilde{B}^{(k)}_v)$. Observe that these new objects are simply $\bar{B}_v$, $\tilde{A}_v$ and $\tilde{U}_v$ defined in (15) and (19), only h has been replaced by $\frac{h}{k}$. Making use of these definitions we have the following generalization of Proposition 11.

Lemma 17 *Suppose $k > 0$ is an integer and $q \in \{0\} \oplus \left(\bigoplus_{l=1}^{nk} \mathcal{R}^{c_v} \right)$. Then all solutions $\tilde{v} \in \bigoplus_{l=0}^{nk-1} L_2[0, \frac{h}{k})$ to*

$$q = \pi_{nk} S_{\frac{h}{k}} P_v \Lambda^{-1}_{\frac{h}{k}} \pi^*_{nk-1} \tilde{v}$$

are given by $\tilde{v} = \tilde{U}^{(k)}_v \bar{v} + \tilde{v}^{\ddagger}$, with $\tilde{v}^{\ddagger} \in \bigoplus_{l=0}^{nk-1} \mathcal{N}(\tilde{B}^{(k)}_v)$ and $\bar{v} \in \bigoplus_{l=0}^{nk-1} \mathcal{R}^{b_v}$ satisfying,

$$(q_1, \ldots, q_{nk}) = \bar{P}^{(k)}_v \bar{v},$$

where

$$\bar{P}^{(k)}_v := \begin{bmatrix} C_v \bar{B}^{(k)}_v & 0 & \cdots & 0 \\ C_v \tilde{A}^{(k)}_v \bar{B}^{(k)}_v & \ddots & & 0 \\ \vdots & \ddots & & \vdots \\ C_v (\tilde{A}^{(k)}_v)^{nk-1} \bar{B}^{(k)}_v & \cdots & C_v \tilde{A}^{(k)}_v \bar{B}^{(k)}_v & C_v \bar{B}^{(k)}_v \end{bmatrix}. \tag{37}$$

Proof This result follows immediately from the proof of Proposition 11 simply replacing h with $\frac{h}{k}$ and n with nk. ■

Using this lemma we can now prove the following key result, which allows us to generalize the invalidation results of the preceding section. For convenience define the matrix

$$J_v^{(k)} := [I\ 0\ \cdots\ 0]$$

which is in $\mathcal{R}^{c_v \times c_v k}$.

Proposition 18 *Suppose $k > 0$ is an integer and $q \in \{0\} \oplus \left(\bigoplus_{l=1}^{n} \mathcal{R}^{c_v} \right)$. Then all solutions $\tilde{v} \in \bigoplus_{l=0}^{nk-1} L_2[0, \frac{h}{k})$ to*

$$q = \pi_n S_h P_v \Lambda_{\frac{h}{k}}^{-1} \pi_{nk-1}^* \tilde{v},$$

are given by $\tilde{v} = \tilde{U}_v^{(k)} \bar{v} + \tilde{v}^\ddagger$, where $\tilde{v}^\ddagger \in \bigoplus_{l=0}^{nk-1} \mathcal{N}(\tilde{B}_v^{(k)})$, and $\bar{v} \in \bigoplus_{l=0}^{nk-1} \mathcal{R}^{b_v}$ satisfying

$$(q_1, \ldots, q_n) = \bar{J}_v^{(k)} \bar{P}_v^{(k)} \bar{v}.$$

The matrix $\bar{P}_v^{(k)}$ is defined in (37) and the matrix $\bar{J}_v^{(k)} := diag(J_v^{(k)}, \ldots, J_v^{(k)}) \in \mathcal{R}^{nc_v \times nc_v k}$.

Proof We start with the following equalities which follow from (36):

$$\begin{aligned} q &= \pi_n S_h P_v \Lambda_{\frac{h}{k}} \pi_{nk-1}^* \tilde{v} = \pi_n \Gamma_k S_{\frac{h}{k}} P_v \Lambda_{\frac{h}{k}} \pi_{nk-1}^* \tilde{v} \\ &= \pi_n \Gamma_k \pi_{nk-1}^* \pi_{nk-1} S_{\frac{h}{k}} P_v \Lambda_{\frac{h}{k}} \pi_{nk-1}^* \tilde{v}. \end{aligned}$$

We now rewrite the latter equation as a condition in two equations: $\tilde{v}$ is a solution to the above equation if and only if there exists $r \in \mathcal{R}^{nk}$ so that

$$\begin{aligned} r &= \pi_{nk-1} S_{\frac{h}{k}} P_v \Lambda_{\frac{h}{k}} \pi_{nk-1}^* \tilde{v} \quad \text{and} \\ q &= \pi_n \Gamma_k \pi_{nk-1}^* r \end{aligned} \tag{38}$$

are both satisfied. From Lemma 17 we know $\tilde{v}$ is a solution to the first equation exactly when it can be written as $\tilde{v} = \tilde{U}_v^{(k)} \bar{v} + \tilde{v}^\ddagger$, with $\tilde{v}^\ddagger \in \bigoplus_{l=0}^{n-1} \mathcal{N}(\tilde{B}_v^{(k)})$ and $\bar{v} \in \bigoplus_{l=0}^{nk-1} \mathcal{R}^{b_v}$ such that $r = \bar{P}_v^{(k)} \bar{v}$. It is routine to verify that $\pi_n \Gamma_k \pi_{nk}^* = \mathrm{diag}(J_v^{(k)}, \bar{J}_v^{(k)})$. Using these two facts, and the constraint that $r_0 = 0$, it is straightforward to convert the conditions in (38) to those in the claim. ■

The following result is a version of Theorem 15 where the degree of anticipation of the perturbation can be chosen as close to zero as desired.

Theorem 19 *Suppose* $u \in L_2[0,\infty)$, $y \in \bigoplus_{l=0}^{n} \mathcal{R}^{c_v}$, $k > 0$ *is an integer, and define* $z = P_z u$. *Then the model in Figure 3 is* not invalidated *with respect to* $\frac{h}{k}$*-anticipatory perturbations if and only if there exist vectors* $\bar{v} \in \bigoplus_{l=0}^{nk-1} \mathcal{R}^{b_v}$ *and* $\bar{w} \in \bigoplus_{l=0}^{n} \mathcal{R}^{b_w}$, *with* $|\bar{w}|_2 \leqslant 1$, *satisfying,*

$$y - \pi_n S_h P_y u = [\bar{P}_w \;\; \bar{J}_v^{(k)} \bar{P}_v^{(k)}] \begin{bmatrix} \bar{w} \\ \bar{v} \end{bmatrix} \quad \text{and} \quad \sum_{k=0}^{l-1} |\bar{v}_k|_2^2 \leqslant \|\Pi_{l\frac{h}{k}} z\|_2 \;\; \text{for } 1 \leqslant l \leqslant nk.$$

The proof of this theorem essentially follows that of Theorem 15 using Proposition 18 in place of Proposition 11, and is therefore not included. Also, we can modify proof of Theorem 16 in a similar way to get the following result.

Theorem 20 *Suppose* $u \in L_2[0,\infty)$, $y \in \bigoplus_{l=0}^{n} \mathcal{R}^{c_v}$, $k > 0$ *is an integer, and define* $z = P_z u$ *and* $\tilde{z} = \pi_{nk-1} \Lambda_{\frac{h}{k}} z$. *Then the model in Figure 3 is* not invalidated *with respect to* $\frac{h}{k}$*-anticipatory,* $\frac{h}{k}$*-periodic, perturbations if and only if there exist vectors,* $\bar{v} \in \bigoplus_{l=0}^{nk-1} \mathcal{R}^{b_v}$ *and* $\bar{w} \in \bigoplus_{l=0}^{n} \mathcal{R}^{b_w}$, *with* $|\bar{w}|_2 \leqslant 1$, *satisfying,*

$$y - \pi_n S_h P_y u = [\bar{P}_w \;\; \bar{J}_v^{(k)} \bar{P}_v^{(k)}] \begin{bmatrix} \bar{w} \\ \bar{v} \end{bmatrix} \quad \text{and} \quad \bar{V}^* \bar{V} \leqslant \tilde{Z}_{\frac{h}{k}}^* \tilde{Z}_{\frac{h}{k}},$$

where $\bar{V}$ *and* $\tilde{Z}_{\frac{h}{k}}$ *are defined from* $\bar{v}$ *and* $\tilde{z}$ *respectively, as in (4).*

The last two results provide a method by which to invalidate with respect to perturbation sets that can be varied by choosing the parameter k. The next result states that if k gets large, the above conditions closely approximate the conditions for invalidation to causal and LTI uncertainty sets.

Theorem 21 *Suppose* $u \in L_2[0,\infty)$, $y \in \bigoplus_{l=0}^{n} \mathcal{R}^{c_v}$.

(i) If the model in Figure 3 can be invalidated with respect to causal *perturbations, then for k sufficiently large it can be invalidated with respect to $\frac{h}{k}$-anticipatory perturbations.*

(i) If the model in Figure 3 can be invalidated with respect to causal, LTI, *perturbations, then for k sufficiently large it can be invalidated with respect to $\frac{h}{k}$-anticipatory, $\frac{h}{k}$-periodic, perturbations.*

Proof

Part (i): Suppose the model is not invalidated to $\frac{h}{k}$-anticipatory perturbations for every $k \geqslant 1$. Then there exists a sequence of operators Δ_k, each being $\frac{h}{k}$-anticipatory with $\|\Delta_k\| \leqslant 1$, and a sequence $w_k \in L_2(-\infty, \infty)$, norm bounded by one, that satisfy,

$$y - \pi_n S_h P_y u = \pi_n S_h P_w w_k + \pi_n S_h P_v \Delta_k P_z u. \tag{39}$$

By Lemma 12 and Proposition 13, without loss of generality, we may assume that the sequence w_k lies in a finite dimensional subspace of $L_2(-\infty, \infty)$; thus by compactness we can further assume it converges to some element w in $L_2(-\infty, \infty)$. Using this convergence and (39) the following limit is therefore well-defined;

$$\lim_{k \to \infty} \pi_n S_h P_v \Delta_k z =: r \tag{40}$$

where $z := P_z u$.

Now the sequence Δ_k is uniformly bounded and therefore we assume, without losing generality, that it converges weak* to some operator Δ. Using the basic definition of weak* convergence and (40) it is routine to show that Δ satisfies $r = \pi_n S_h P_v \Delta z$. Therefore, using (40) and (39) we conclude

$$y - \pi_n S_h P_y u = \pi_n S_h P_w w + \pi_n S_h P_v \Delta P_z u.$$

But by Lemma 5 (b) the operator Δ is causal. Therefore the model is not invalidated with respect to causal perturbations.

Part (ii): This has a nearly identical proof, only we take a sequence Δ_k of elements that are both $\frac{h}{k}$-anticipatory and $\frac{h}{k}$-periodic. By Lemma 5 the weak* limit constructed, Δ, is both causal and LTI. ■

The results of this section clearly illustrate that, in the limit as $k \to \infty$ we are heading towards an infinite dimensional characterization of invalidation with respect to causal and causal, LTI, perturbations. We will not elaborate further on the resulting infinite dimensional optimization problem here, except to say that it is convex. The finite dimensional approximations given here are of interest as they lead to the computable algorithms in the next section.

It is of interest to quantify the rate of convergence of these finite dimensional problems to the infinite dimensional one. We leave a more formal study of this area to future research.

4 Computational Model Validation Algorithm

4.1 Formulation of the Optimization Problem

We now formulate the model validation matrix optimization problem that enables us to make use of the conditions constructed in Theorem 16. From this point on we concentrate on the h-anticipatory, h-periodic, case, and its relation to LTI model validation. The purely h-anticipatory case can be formulated in a similar manner. Here we explicitly include the variable γ to formulate a search for the smallest perturbation and noise accounting for the datum.

In the following the matrices $\bar{P}_w$, $\bar{P}_v$ are those defined in (28) and (22). The matrices $\tilde{Z}_h^*\tilde{Z}_h$ and $\bar{V}^*\bar{V}$ are calculated from $z(t)$ and $\bar{v}$ as in (4). For simplicity we define $\bar{r}$ as the residual, calculated at the sample instants over the interval $[0, nh]$ by,

$$\bar{r} = y - \pi_n S_h P_y \Pi_{nh}^* u.$$

The following optimization problem is therefore over $\mathcal{R}^{nb_v} \oplus \mathcal{R}^{(n+1)b_w} \oplus \mathcal{R}$.

Problem 22 *(Minimum Norm Optimization)*

$$\hat{\gamma} := \min_{\bar{v},\bar{w},\gamma} \gamma,$$

subject to,

$$\bar{r} = \begin{bmatrix} \bar{P}_w & \bar{P}_v \end{bmatrix} \begin{bmatrix} \bar{w} \\ \bar{v} \end{bmatrix}, \tag{41}$$

$$\bar{V}^*\bar{V} \leqslant \gamma^2 \tilde{Z}_h^*\tilde{Z}_h, \tag{42}$$

and

$$\bar{w}^*\bar{w} \leqslant \gamma^2. \tag{43}$$

This is a convex, non-differentiable optimization problem which can be solved with a number of algorithms. The convexity arises from the fact that the problem formulation results in $\tilde{Z}_h^* \tilde{Z}_h$ being a fixed matrix. A variety of methods are available for solving such problems. For example; ellipsoidal algorithms, cutting plane algorithms, and linear matrix inequality (LMI) approaches [39, 40, 41]. Appendix C provides additional details on an LMI based approach.

We now formally state the relationship between the above optimization problem and the model validation problem. This is a simple extension of Theorem 16 and we therefore omit the proof.

Proposition 23 *Given $\hat{\gamma}$, the solution to Problem 22: If $\hat{\gamma} > 1$, then the model given in Figure 3 is* invalidated *with respect to h-anticipatory, h-periodic, perturbations, Δ, and $w(t) \in L_2(-\infty, \infty)$, satisfying $\|\Delta\|_{L_2 \to L_2} \leqslant 1$ and $\|w(t)\|_2 \leqslant 1$.*

Note that we could use the results of Section 3.3.3 to state the same result for $\frac{h}{k}$-anticipatory and $\frac{h}{k}$-periodic perturbations. Instead we will state the result which is applicable to most of the models of interest.

Proposition 24 *Given $\hat{\gamma}$, the solution to Problem 22: If $\hat{\gamma} > 1$, then the model given in Figure 3 is* invalidated *with respect to causal, LTI, perturbations, Δ, and $w(t) \in L_2(-\infty, \infty)$, satisfying $\|\Delta\|_{L_2 \to L_2} \leqslant 1$ and $\|w(t)\|_2 \leqslant 1$.*

This follows simply from the fact that the class of h-anticipatory, h-periodic, perturbations includes all causal, LTI, perturbations. Proposition 24 forms the basis of the algorithm in the following section.

4.2 A Practical Model Invalidation Algorithm

We can now apply the above optimization techniques to give an algorithm for model invalidation. The approach involves undersampling the datum to give smaller optimization problems. For notational simplicity we assume that the number of points in the output datum is a power of two. Here we have chosen to form an algorithm based on subsets of the available datum. The datum is further sampled to reduce the number of points and the lifting operation is applied to test the existence of an h-anticipatory Δ, where h is also the period of the selected data subset. We further have the option of applying successively faster lifting operators around the perturbation (using the theory in Section 3.3.3) to more closely approximate the causal, LTI, test. Note that we present only the LTI case — the LTV case can be similarly formulated, using Theorem 15 rather than Theorem 16.

Algorithm 25 (Invalidation with respect to LTI, causal, perturbations)

Given: an experimental datum, (y_k,$u(t)$), $k = 0, \ldots, 2^q - 1$, on the interval $[0, T]$, and a perturbation model, P.

1. *Set an integer $l = 1$ and select decimation factor, $q_l < q$, such that 2^{q_l} represents a small optimization problem.*
2. *Decimate the datum to give a new datum of length 2^{q_l}: (y_{k_l},$u(t)$), where $k_l = 0, p, 2p, 3p, \ldots, (2^q - 1)p$ and $p = 2^{q-q_l}$. This gives $h_l = T/(2^{q_l} - 1)$.*
3. *Calculate $\hat{\gamma}_l$ for the datum (y_{k_l},$u(t)$) via the optimization given in Problem 22.*
4. *If $\hat{\gamma}_l > 1$ then the datum invalidates the model. (stop).*
5. *(optional) Select an integer $k > 0$.*
   - 5a. *Solve the optimization problem arising from Theorem 20 and denote the result by $\hat{\gamma}_l^k$. The output sample period remains $h_l = T/(2^{q_l} - 1)$. The lifting is performed using $\frac{h_l}{k}$ in place of h_l.*
   - 5b. *If $\hat{\gamma}_l^k > 1$ the datum invalidates the model (stop).*
   - 5c. *Increase k and go to step 5a* <u>or</u> *continue with step 6.*
6. *If $q_l = q$ then the datum does not invalidate the model (stop).*
7. *Increment l and q_l and go to step 2.*

Note that at each iteration, the new decimated datum, (y_{k_l},$u(t)$), contains all previously tested decimated data as a subset. Therefore $\hat{\gamma}_l$, $l = 1, \ldots$ is non-decreasing. The algorithm will therefore find a particular $\hat{l}$ such that $\hat{\gamma}_{\hat{l}} > 1$, or will exhaust all of the available data. Proposition 24 implies that if we find such a $\hat{l}$ then the model is invalidated by the datum. Note that we also have the option of using a faster lifting operation ($\frac{h}{k}$ instead of h) around the perturbation in order to more closely approximate the test for LTI, causal, perturbations. The choice of whether to use the optional step

5 and the decision at step 5c is based whether or not improving the approximation to the LTI, causal, case is likely to result in $\hat{\gamma}_l^k > 1$. There will be problem dependent computational consequences in selecting between increasing k or increasing l and resampling the datum.

The most significant feature of this approach (with or without the optional step 5) is that it begins with small optimization problems. If only a small amount of data is required to invalidate the model, the algorithm will return this result quickly.

5 A Simulation Example

We give a simulation based example to illustrate the approach on practical problems. The "experimental" datum has been generated by the "true" system,

$$P_{true} = \left(\frac{10.5}{0.22s+1}\right)\left(\frac{-0.075s+2}{0.075s+2}\right)\left(\frac{1000}{s^2+10s+1000}\right).$$

For the model validation problem we will consider the following perturbed model,

$$y(t) = (I + W_\Delta \Delta) P_{nom}\, u(t) + W_d\, w(t),$$

where, $\|\Delta\|_{L_2 \to L_2} \leqslant 1$ and $w(t) \in BL_2$. The nominal model is given by,

$$P_{nom} = \frac{10}{0.2s+1}.$$

Note that the model has errors in the gain and pole positions and does not account for some additional phase or a higher frequency resonant pole pair. The multiplicative perturbation weight is,

$$W_\Delta = \frac{0.075(1+1.5s)}{1+0.025s},$$

and is intended to cover the dynamic errors between P_{true} and P_{nom}. The output disturbance weight, W_d, reflects the size and frequency dependency of the noise and disturbances, and is given by,

$$W_d = \frac{0.025(1+0.01s)}{1+s}.$$

As this is a simulation, it is possible to calculate the actual relative error between P_{true} and P_{nom} and compare it to W_Δ. This is done in Figure 7.

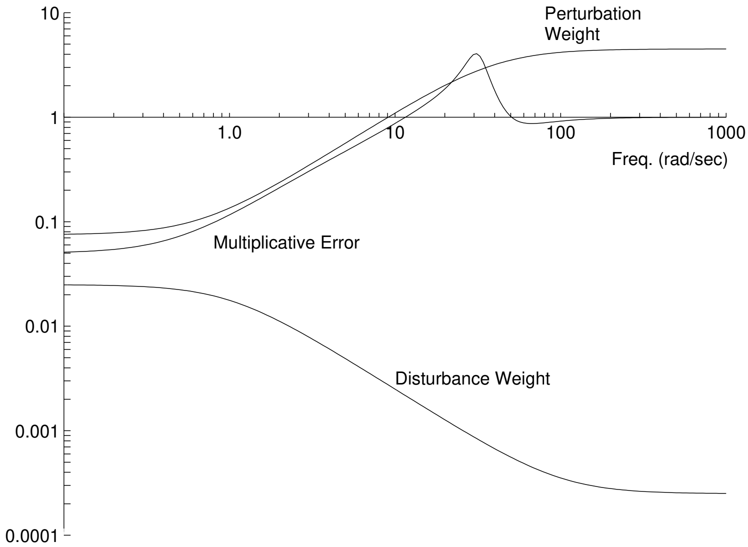

Figure 7: Weighting functions in example robust control model: perturbation weight, W_Δ, and disturbance/noise weight, W_d. Also shown is the actual relative error between P_{true} and P_{nom}

Note that W_Δ does not overbound the actual relative error meaning that this model cannot account for every system behavior. The issue here is whether or not it will account for a given experiment.

To conduct the simulation "experiment", a series of steps were introduced to the system via a zero-order hold. An anti-aliasing filter,

$$F = \frac{20\pi}{s + 20\pi},$$

prefiltered the data before it was sampled with period, $h = 0.01$. The experimental datum consisted of 512 points and is shown if Figure 8. The nominal system response, $P_{nom}\, u(t)$, is also shown (smooth curve).

Algorithm 25 was applied without using the faster lifting approach (step *5*), and the datum was undersampled at periods: $h_1 = 0.64$, $h_2 = 0.32$, and $h_3 = 0.16$ seconds. In the notation of Algorithm 25 this corresponds to $q = 9$ and $q_1 = 3$, $q_2 = 4$, $q_3 = 5$. For each set of undersampled data, the minimum norm Δ and minimum norm $w(t)$ generating that sampled data were calculated. The results for each case, are shown in Table 1. The number of sample points being considered in each case was very small compared to the original datum, leading to optimization problems of

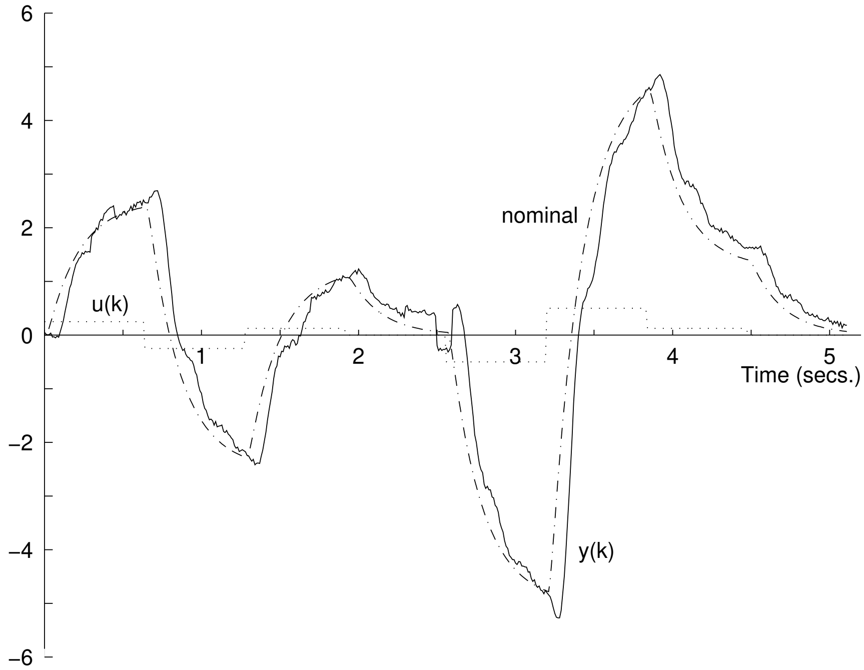

Figure 8: Input/output datum: 512 samples at $h = 0.01$. Also shown is the nominal system response.

manageable size.

l	# datum points	subsampled period (sec.)	subsampled freq. (rad/sec)	$\hat{\gamma}_l$
1	8	0.64	9.82	0.021
2	16	0.32	19.64	0.690
3	32	0.16	39.27	1.293

Table 1: Simulation example validation analysis results

Note that for $h_3 = 0.16$, $\hat{\gamma}_3$ is greater than one, meaning that there is no perturbation $\Delta : L_2 \rightarrow L_2$, and $w(t) \in L_2$ of norm less than one going through the same sample points. This experiment therefore invalidates the model. Note that only a small subset of the experimental datum was required to invalidate the model. Consequently the convex optimization problems required were small (of dimension comparable to the size of each undersampled datum). The observant reader will also note that the sampling frequency required to invalidate the datum is very close to the frequency range where the perturbation weight is unable to cover the actual relative model error. It is possible to calculate the signals in the model that correspond to $\hat{\gamma}$ although these apply to the model, rather than the physical system and do not necessarily have any interpretation as signals within the physical system.

6 An Experimental Example

In this section we apply the model validation procedure of Algorithm 25, and the LMI algorithm of the preceding section, to assess the quality of a perturbation model for a laboratory thermal heating experiment.

Figure 9 illustrates the experimental configuration. The system consists of a 300 Watt lamp suspended 2 inches above a thin metal plate. A thermocouple, mounted on the underside of the plate, and interfaced via an A/D board, provides a measurement of the surface temperature. A thyristor based power amplifier, driven by a D/A board, is used to effect computer control of the lamp. A Macintosh, running LabView, is used for control and data acquisition.

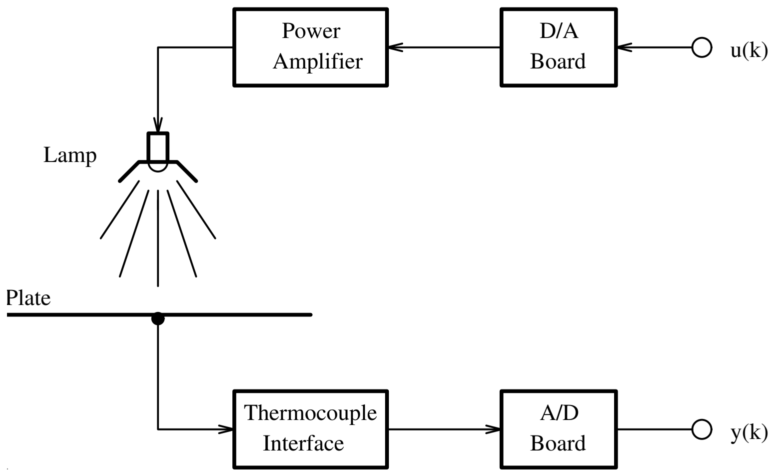

Figure 9: Heat experiment configuration

The full uncertainty model used for this experimental setup is illustrated in Figure 11, which has a multiplicative uncertainty structure, and clearly fits the model of Figure 3. The block, NL, denotes a static nonlinearity, due mostly to the power amplifier. The output of NL is approximately $10 \sin((2\pi/40)\, u)$, although a more precise look-up table is used below. The LTI part of the nominal model is,

$$P(s) = \frac{2.15}{80s + 1}.$$

This has been obtained by a combination of ARX methods and matching step response data. A weighted multiplicative perturbation, Δ, and an output disturbance signal, $d(t)$, provide a model of our uncertainty about the true system. The associated weights are,

$$W_\Delta(s) = \frac{0.1(150s + 1)}{10s + 1}, \quad \text{and} \quad W_d = 0.6.$$

The noise weight, W_d, has been determined by measuring the 2-norm of an identical thermocouple at constant temperature, over the same experiment duration. The perturbation weight, W_Δ, is a normalization factor has been obtained from ad-hoc estimates of the model accuracy. Figure 10 shows the nominal plant model and the perturbation and noise weights.

The filter, $F(s)$, is a cascade of our model for the thermocouple interface and a data filter:

$$F(s) = \frac{1}{15.92s + 1}.$$

In the experiments described here, the sampling period used for data acquisition was 2 seconds. Applying the subsampling algorithm (Algorithm 25) leads to sampling periods h_l that are significantly larger.

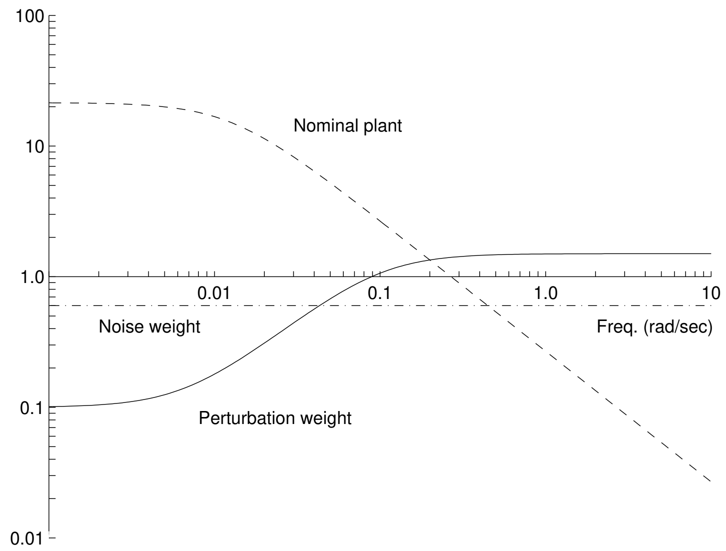

Figure 10: Nominal model, perturbation, and noise weights

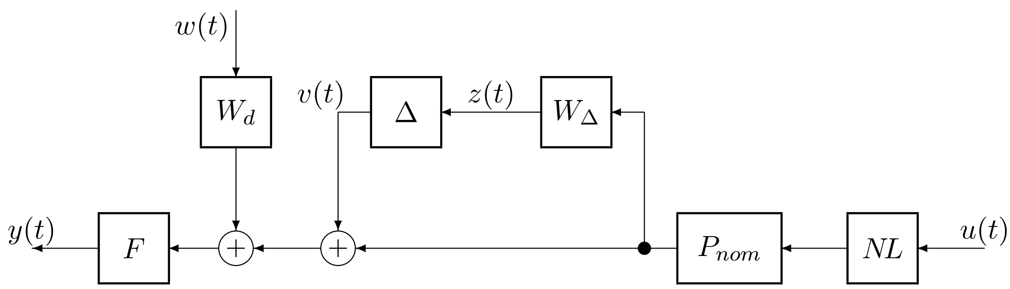

Figure 11: Perturbation model of the heat system

The objective is to assess the quality of this model with respect to an experiment. In particular, we would like to determine, based on observed data, whether $\|\Delta\|_{L_2 \to L_2} \leqslant 1$ is a valid assumption for control design. The assumed bound on the disturbance, $\|w(t)\|_2 \leqslant \gamma = 1$, is applied as a constraint. Recall that W_d weights the effect of $w(t)$ on the output.

The experimental input, $u(t)$, consists of a series of voltage steps. Figure 12 shows the sampled input signal, u_k; the sampled output measurements, y_k; the response of the nominal model; and the residual, r. The residual is the difference between the experimentally observed data y_k, and the output of the nominal model $S_h F P_{nom} NL\, u$, with $\Delta = w = 0$. It is significant and, in fact, $\|r\|_2 = 24.21$. This input signal was not used in the original identification, which is why there is such an large model error.

Note that if $F(s)$ is a low-pass filter, with a high bandwidth, then there is almost no penalty applied to $\|w(t)\|_2$. The disturbance, w, can be used to generate spikes at the appropriate sample times. In such cases, subsampled optimization problems would yield very low values of $\hat{\gamma}_l$. A large portion of the data set, leading to a high dimensional optimization problem, would have to be examined to obtain a realistic estimate of $\hat{\gamma}$. For this reason we have selected $F(s)$ to have a lower bandwidth than is actually the case for the experiment. It is still higher than the bandwidth of the plant and does not appreciably affect the responses.

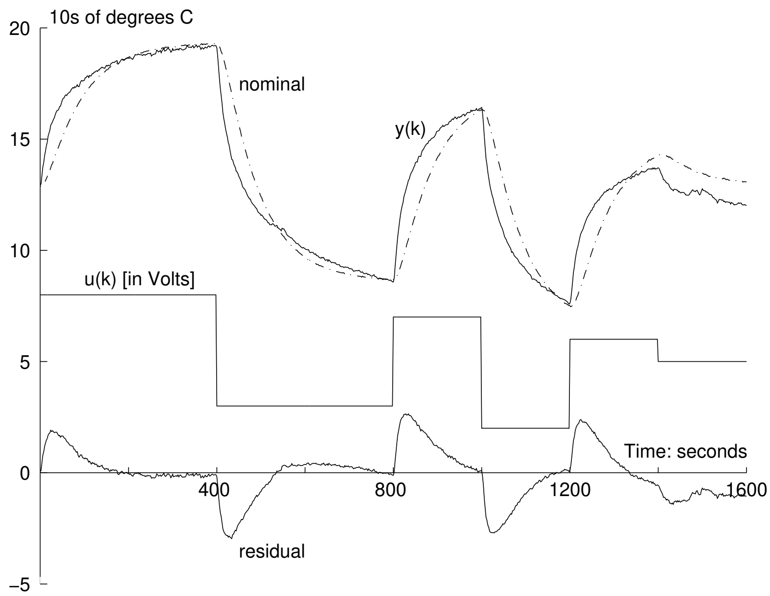

Figure 12: Measured datum and residual

l	# datum points	subsampled period (sec.)	$\hat{\gamma}_l$	$\|r_l\|$
1	9	200	0.228	22.76
2	17	100	0.420	20.73
3	24	68	0.780	16.29
4	33	50	0.945	12.41
5	41	40	1.07	9.85
6	64	25	1.20	6.56

Table 2: Experimental example validation analysis results

The subsampling approach in Algorithm 25, was applied and the results for various subsampling frequencies are shown in Table 2. To facilitate the discussion, each subsampled problem is indexed by l.

Two quantities are useful in assessing the model validation question. The first is $\hat{\gamma}_l$, the size of the minimum $\|\Delta\|_{L_2 \to L_2}$, accounting for the datum at the subsampled points. This is a lower bound on the minimum $\|\Delta\|_{L_2 \to L_2}$ required to account for the observation over the entire data set, since we are using the partial data record (y_{kl}, u_{kl}).

The quantity, $\|r_l\|$, is the component of the residual, still unaccounted for by w_l, and Δ_l, the smallest noise and perturbation matching the lth datum subset. More formally,

$$r_l = y - S_h(P_w w_l + (P_v \Delta_l P_z + P_u)u).$$

Note that to do this it is necessary, at each step, l, to explicitly calculate the effect of w_l and Δ_l on the output. Initially, $l = 0$, $w_l = 0$, $\Delta_l = 0$, and $\|r_l\| = \|r\|$. As l increments, w_l and Δ_l account for progressively more of the residual, to the point where if $h_l = h$, $r_l = 0$. The quantity $\|r_l\|$ therefore gives an estimate of how close each subproblem is to accounting for the entire data set. It is a particularly useful quantity, because it is typically not computationally feasible to perform the exact LMI calculation, corresponding to Theorem 16, for the entire datum; however r_l is easily computed.

We want to determine whether the assumption that $\|\Delta\|_{L_2 \to L_2} \leqslant 1$ is valid, and, from Table 2 ($l = 5$), we can see that this datum has invalidated the model. Note that we need only examine 41 of the 800 points in the datum to make this determination; furthermore 800 points would be an infeasibly expensive computation with our current LMI implementation. The calculations illustrate more than just a yes/no determination of the model validation question. Note that the residual is of size, $\|r\| = 24.21$, and that, at most, the disturbance input, $w(t) \in BL_2$, can account for $\|F(s)W_d\, w(t)\| \leqslant 0.6$ of this residual. Therefore the perturbation, Δ, accounts for a significant component of the residual, and although $\|\Delta\|_{L_2 \to L_2} > 1$, we may deduce from its growth rate of $\hat{\gamma}_l$ (and the decay rate of $\|r_l\|$) in the subsampled problems, that it is could reasonably be within a factor of two of being correct for the datum.

7 Conclusions

We have developed a theoretical and computational framework for treating a practically motivated robust control model validation problem — continuous time models with discrete-time measurement data. The effects of the continuous-time unknown model elements, Δ and w, are observed through LTI systems. This enables the problem of finding the smallest norm Δ, and w, accounting for the datum to be considered as a finite dimensional problem.

Applying the lifting theory allows the calculation of the smallest h-periodic and h-anticipatory Δ accounting for the datum. This gives a lower bound on the smallest norm LTI, causal, Δ accounting for the datum which can be used for invalidation of the model. The lifting operators applied around Δ are not constrained to be at the same period as the output sampler, S_h. By using successively faster lifting operators (as given in Section 3.3.3) the bound can be made arbitrarily close to the LTI, causal, case. There is a computational penalty in doing this as the resulting matrix characterization increases in dimension.

This approach differs significantly from that of discretizing the model and applying a discrete-time model validation test. We provide a means of calculating (or bounding) the size of the smallest continuous Δ and continuous w accounting for the discrete-time datum. Therefore we require no assumptions about the sample period in considering the continuous-time model.

The framework presented here assumed that the samples were regularly spaced. This is by far the most common case although it is not essential; irregular sample spacing would require a recalculation of the finite dimensional subspace representations for each time step. It should also be noted that for a closed-loop validation problem, the framework can be modified to deal with the case where the sampled-data controller is not using the same period as the output sampler, S_h.

Convexity of the resulting optimization problem relies on knowing the input $z(t)$, to the perturbation Δ. Unknown signals, $w(t)$ are constrained to act upon the output of Δ. This model structure is relatively common although not the most general. The general perturbation structure problem is of practical and theoretical interest and will be the subject of future research.

This work provides a framework for experimentally assessing perturbation models. For mathematical precision, the problem is formulated as a yes/no hypothesis test. The real value of the approach comes from the engineering interpretation given to the intermediate subsampled solutions and the size of the remaining residual. In the above we have mentioned applying these techniques to system identification. They can also be applied to fault detection, where the gradual increase of $\hat{\gamma}$ may be interpreted as a deterioration process, and a step change in $\hat{\gamma}$ may be interpreted as a component failure. In a changing environment, the model validation approach can be used to indicate the necessity of reidentifying the system. The practical applications of such schemes are currently under investigation.

Acknowledgements

Roy Smith is supported by NSF grant ECS-93-8917 and Geir Dullerud is supported by AFOSR.

References

[1] L. Ljung, *System Identification, Theory for the User.* Information and System Sciences Series, New Jersey: Prentice-Hall, 1987.

[2] J. Doyle, "Analysis of feedback systems with structured uncertainties," *IEE Proceedings, Part D*, vol. 133, pp. 45–56, Mar. 1982.

[3] J. Doyle, "Structured uncertainty in control system design," in *Proc. IEEE Control Decision Conf.*, pp. 260–265, 1985.

[4] M. A. Dahleh and J. B. Pearson, Jr., "l^1-optimal feedback controllers for MIMO discrete-time systems," *IEEE Trans. Auto. Control*, vol. AC-32, pp. 314–322, Apr. 1987.

[5] M. Khammash and J. B. Pearson, Jr., "Performance robustness of discrete-time systems with structured uncertainty," *IEEE Trans. Auto. Control*, vol. AC-36, pp. 398–412, Apr. 1991.

[6] M. A. Dahleh and J. B. Pearson, Jr., "l^1-optimal compensators for continuous-time systems," *IEEE Trans. Auto. Control*, vol. AC-32, pp. 889–895, Oct. 1987.

[7] The MathWorks, Inc., Natick, MA, *μ-Analysis and Synthesis Toolbox (μ-Tools)*, 1991.

[8] G. Goodwin and M. Salgado, "Quantification of uncertainty in estimation using an embedding principle," in *Proc. Amer. Control Conf.*, 1989.

[9] G. Goodwin, B. Ninness, and M. Salgado, "Quantification of uncertainty in estimation," in *Proc. Amer. Control Conf.*, pp. 2400–2405, 1990.

[10] B. M. Ninness and G. C. Goodwin, "Robust frequency response estimation accounting for noise and undermodeling," in *Proc. Amer. Control Conf.*, pp. 2847–2851, 1992.

[11] H. Hjalmarsson and L. Ljung, "Estimating model variance in the case of undermodeling," *IEEE Trans. Auto. Control*, vol. 37, pp. 1004–1008, July 1992.

[12] P. J. Parker and R. R. Bitmead, "Adaptive frequency response identification," in *Proc. IEEE Control Decision Conf.*, pp. 348–353, 1987.

[13] A. Helmicki, C. Jacobson, and C. Nett, "H_∞ identification of stable LSI systems: A scheme with direct application to controller design," in *Proc. Amer. Control Conf.*, pp. 1428–1434, 1989.

[14] A. J. Helmicki, C. A. Jacobson, and C. N. Nett, "Control oriented system identification: A worst-case/deterministic approach in H_∞," *IEEE Trans. Auto. Control*, pp. 1163–1176, 1991.

[15] P. Mäkilä and J. Partington, "Robust approximation and identification in H^∞," *Proc. Amer. Control Conf.*, pp. 70–76, 1991.

[16] P. Mäkilä, "Laguerre methods and H^∞ identification of continuous-time systems," *Int. J. of Control*, vol. 53, pp. 689–707, 1991.

[17] G. Gu and P. P. Khargonekar, "Linear and nonlinear algorithms for identification in H^∞ with error bounds," in *Proc. Amer. Control Conf.*, pp. 64–69, 1991.

[18] Z. Zang, R. R. Bitmead, and M. Gevers, "H_2 iterative model refinement and control robustness enhancement," in *Proc. IEEE Control Decision Conf.*, pp. 279–284, 1991.

[19] W. S. Lee, B. D. O. Anderson, R. L. Kosut, and I. M. Y. Mareels, "A new approach to adaptive robust control," *Int. J. of Adapt. Control & Sig. Proc.*, vol. 7, pp. 183–211, 1993.

[20] R. J. P. Schrama, "Accurate identification for control: the necessity of an iterative scheme," *IEEE Trans. Auto. Control*, vol. 37, pp. 991–994, July 1992.

[21] P. M. J. Van den Hof and R. J. P. Schrama, "Identification and control — closed loop issues," in *10th IFAC Symp. on Syst. Ident.*, pp. 2.001–2.014, 1994.

[22] R. S. Smith and J. Doyle, "Model invalidation — a connection between robust control and identification," in *Proc. Amer. Control Conf.*, pp. 1435–1440, 1989.

[23] R. S. Smith and J. C. Doyle, "Model validation: A connection between robust control and identification," *IEEE Trans. Auto. Control*, vol. 37, pp. 942–952, July 1992.

[24] J. M. Krause, "Stability margins with real parameter uncertainty: Test data implications," in *Proc. Amer. Control Conf.*, pp. 1441–1445, 1989.

[25] K. Poolla, P. Khargonekar, A. Tikku, J. Krause, and K. Nagpal, "A time-domain approach to model validation," in *Proc. Amer. Control Conf.*, pp. 313–317, 1992.

[26] T. Zhou and H. Kimura, "Input-output extrapolation-minimization theorem and its application to model validation and robust identification," in *The Modeling of Uncertainty in Control: Proceedings of the 1992 Santa Barbara Workshop* (R. Smith and M. Dahleh, eds.), pp. 127–137, Springer-Verlag, 1994.

[27] K. Poolla, P. Khargonekar, A. Tikku, J. Krause, and K. Nagpal, "A time-domain approach to model validation," *IEEE Trans. Auto. Control*, vol. 39, no. 5, pp. 951–959, 1994.

[28] B. A. Bamieh, J. J. Boyd Pearson, B. A. Francis, and A. Tannenbaum, "A lifting technique for linear periodic systems with applications to sampled-data control," *Syst. and Control Letters*, vol. 8, 1991.

[29] B. A. Bamieh and J. J. Boyd Pearson, "A general framework for linear periodic systems with applications to H_∞ sampled-data control," *IEEE Trans. Auto. Control*, vol. 37, no. 4, pp. 418–435, 1992.

[30] Y. Yamamoto, "A function space approach to sampled data control systems and tracking problems," *IEEE Trans. Auto. Control*, vol. 39, no. 4, pp. 703–712, 1994.

[31] P. Halmos, *A Hilbert Space Problem Book.* New York: Springer-Verlag, 1982.

[32] C. Foias and A. E. Frazho, *The Commutant-Lifting Approach to Interpolation Problems.* Boston: Birkhauser, 1990.

[33] A. K. Packard and J. C. Doyle, "The complex structured singular value," *Automatica*, vol. 29, no. 1, pp. 71–109, 1993.

[34] A. Packard, K. Zhou, P. Pandey, J. Leonhardson, and G. Balas, "Optimal, constant I/O similarity scaling for full-information and state-feedback control problems," *Syst. and Control Letters*, vol. 19, pp. 271–280, 1992.

[35] L. El Ghaoui, V. Balakrishnan, E. Feron, and S. Boyd, "On maximizing a robustness measure for structured nonlinear perturbations," in *Proc. Amer. Control Conf.*, pp. 2923–2926, 1992.

[36] P. Apkarian, J. P. Chretien, P. Gahinet, and J. M. Biannic, "μ synthesis by *D-K* iterations with constant scaling," in *Proc. Amer. Control Conf.*, pp. 3192–3196, 1993.

[37] S. Thapliyal, Y. Faitakis, and J. Kantor, "A model validation approach to fault detection," in *Proc. Amer. Control Conf.*, pp. 3027–3028, 1994.

[38] R. L. Wheeden and A. Zygmund, *Measure and Integral.* New York: Marcel Dekker, 1981.

[39] S. P. Boyd and C. H. Barratt, *Linear Controller Design, Limits of Performance.* New Jersey: Prentice Hall, 1991.

[40] Y. E. Nesterov and A. S. Nemirovskii, *Interior-Point Polynomial Algorithms in Convex Programming.* Philadelphia: SIAM, 1994.

[41] S. P. Boyd, L. E. Ghaoui, E. Feron, and V. Balakrishnan, *Linear Matrix Inequalities in System and Control Theory.* Philadelphia: SIAM, 1994.

[42] R. Smith and G. Dullerud, "Validation of continuous-time control models using finite experimental data," *IEEE Trans. Auto. Control*, vol. 41, no. 8, pp. 1094–1078, 1996.

[43] C. F. Van Loan, "Computing integrals involving the matrix exponential," *IEEE Trans. Auto. Control*, vol. 23, pp. 395–404, 1978.

[44] S. Boyd and L. El Ghaoui, "Method of centers for minimizing generalized eigenvalues," *Linear Algebra and its Applications*, vol. 188, pp. 63–111, July 1993.

[45] M. K. H. Fan and B. Nekooie, "An algorithm on minimizing generalized eigenvalues with linear matrix inequality constraints," in *Proc. Amer. Control Conf.*, pp. 831–835, 1994.

[46] P. Gahinet and A. Nemirovskii, "General-purpose LMI solvers with benchmarks," in *Proc. IEEE Control Decision Conf.*, pp. 3162–3165, 1993.

[47] J.-P. A. Haeberly and M. L. Overton, "Optimizing eigenvalues of symmetric definite pencils," in *Proc. Amer. Control Conf.*, pp. 836–839, 1994.

A Proof of Technical Lemmas

To prove Lemma 8 we require a number of technical lemmas. Throughout let $T > 0$ be some fixed real number. The first lemma defines a family of functions which have impulsive action.

Lemma 26 *Suppose $w \in L_2[0, T)$, and*

$$\delta^\epsilon(t) := \begin{cases} 1/\epsilon & \text{for } t \in [0, \epsilon) \\ 0 & \text{otherwise} \end{cases} \tag{44}$$

for $\epsilon > 0$. Define $w^\epsilon(t) := \int_0^t \delta^\epsilon(\tau) w(t-\tau)\, d\tau$. Then $\lim_{\epsilon \to 0} \|w - w^\epsilon\|_2 = 0$.

The above result is a particular instance of a more general result on kernels; see, for example, [38, p. 148].

For convenience in the sequel we define two new operators mapping $L_2[0, T)$ to $L_2[0, T)$. Define $\hat{H}_h$ by

$$(\hat{H}_h w)(t) := \int_0^t \delta^h(t-\tau) w(\tau)\, d\tau, \tag{45}$$

where the function δ^h is defined in (44). Also using this function, define the operator $\widehat{S}_h^\epsilon$ via

$$(\widehat{S}_h^\epsilon w)(t) := h \sum_{k=0}^{\lfloor T/h \rfloor} \delta^\epsilon(t - kh) w(t),$$

where $\lfloor T/h \rfloor$ denotes the largest integer that is not greater than T/h.

As ϵ and h get small it is easy to see that the induced norm of $\widehat{S}_h^\epsilon$ becomes large. However, $\hat{H}_h$ has better properties in this regard.

Lemma 27 *For each $h > 0$ the norm $\|\hat{H}_h\| \leqslant 1$.*

Proof Select any $w \in L_2[0, T)$. Then using (45) we have by a standard inequality for convolutions (see, e.g., [38, p. 145]) that $\|\hat{H}_h w\|_2 \leqslant (\int_0^T \delta^\epsilon(\tau)\, d\tau)\|w\|_2 = \|w\|_2$. ■

Lemma 28 *Suppose $w \in L_2[0, T)$ and U is the related convolution operator defined in (14). Then for each $h > 0$ the equality $U\hat{H}_h = \hat{H}_h U$ holds.*

Proof Since both U and $\hat{H}_h$ are convolution operators it is routine to verify that they commute. ■

Before continuing we define the following notation: given $w \in L_2[0,T)$ define $w_{(\tau)}$ for each $\tau \in \mathcal{R}$ by

$$w_{(\tau)}(t) := \begin{cases} u(t-\tau) & \tau \leqslant t < T \\ 0 & \text{otherwise.} \end{cases}$$

Lemma 29 *Suppose* $u \in L_2[0,T)$ *and define* $e_h := \sup_{\tau \in [0,T)} \|\hat{H}_h u_{(\tau)} - u_{(\tau)}\|_2$. *Then* $e_h \stackrel{h \to 0}{\longrightarrow} 0$.

Proof Suppose the contrary: there exist infinite sequences $\tau_k \in [0,T)$ and h_k tending to zero, and $\epsilon > 0$ so that

$$\|\hat{H}_{h_k} u_{(\tau_k)} - u_{(\tau_k)}\|_2 > \epsilon \quad \text{for all } k \geqslant 1. \tag{46}$$

Without loss of generality we assume that τ_k converges to some τ_0 in $[0,T]$. If $\tau_0 = T$ then $\lim_{k\to\infty} \|u_{(\tau_k)}\|_2 = 0$ and therefore (46) is violated. Hence, we assume τ_0 in $[0,T)$.

Now, invoking the triangle inequality, Lemma 27 and the submultiplicative inequality we have

$$\begin{aligned} &\|u_{(\tau_k)} - u_{(\tau_0)}\|_2 + \|u_{(\tau_0)} - u_{(\tau_k)}\|_2 + \|\hat{H}_{h_k} u_{(\tau_0)} - u_{(\tau_0)}\|_2 \\ &\quad \geqslant \|\hat{H}_{h_k}(u_{(\tau_k)} - u_{(\tau_0)})\|_2 + \|u_{(\tau_0)} - u_{(\tau_k)}\|_2 + \|\hat{H}_{h_k} u_{(\tau_0)} - u_{(\tau_0)}\|_2 \\ &\quad \geqslant \|\hat{H}_{h_k} u_{(\tau_k)} - u_{(\tau_k)}\|_2. \end{aligned}$$

By continuity in L_2 (see, e.g., [38, p. 134]) it follows that $\lim_{k\to\infty} \|u_{(\tau_0)} - u_{(\tau_k)}\|_2 = 0$; from Lemma 26 we have $\lim_{k\to\infty} \|\hat{H}_{h_k} u_{(\tau_0)} - u_{(\tau_0)}\|_2 = 0$. So, the LHS above tends to zero as k tends to infinity. But then the RHS contradicts (46). ■

Lemma 30 *Suppose* $u \in L_2[0,T)$, $w(t)$ *is a uniformly continuous function on the interval* $[0,T)$, *and* $h = \frac{T}{n}$ *where* n *is a positive integer. Then*

$$\lim_{\epsilon \to 0} \|U \widehat{S}_h^{\epsilon} w - \Pi_T \Lambda_h^{-1} \pi_{n-1}^* \tilde{U}_h \bar{w}^n\|_2 = 0,$$

where $\tilde{U}_h$ *is defined from* $\tilde{u} = \pi_{n-1} \Lambda_h^{-1} \Pi_T^* u$ *as in (4), and* $\bar{w}^n = h \cdot (w(0), \ldots, w(\,(n-1)h\,)\,)$.

Proof From the definitions we have

$$(\widehat{S}_h^\epsilon w)(t) = h\sum_{k=0}^{n-1}\delta^\epsilon(t-kh)w(t) \quad \text{on } [0,T).$$

Hence,

$$(U\widehat{S}_h^\epsilon w)(t) = \sum_{k=0}^{n-1}\int_0^t u(t-\tau)\delta^\epsilon(\tau-kh)w(\tau)\,d\tau.$$

So, by applying Lemma 26 and a routine argument based on the continuity of $w(t)$ we have

$$U\widehat{S}_h^\epsilon w \stackrel{\epsilon\to 0}{\longrightarrow} h\sum_{k=0}^{n-1} w(kh)u_{(kh)} \quad \text{in } L_2[0,T). \tag{47}$$

It is straightforward to verify that the RHS=$\Pi_T\Lambda_h^{-1}\pi_{n-1}^*\tilde{U}_h\bar{w}^n$ ∎

Lemma 31 *Suppose w is a uniformly continuous function on the interval $[0,T)$. Then*

$$\lim_{h\to 0}\lim_{\epsilon\to 0}\|(I-\hat{H}_h\widehat{S}_h^\epsilon)w\|_2 = 0.$$

Proof For $0<\epsilon<h$ we have

$$(\hat{H}_h\widehat{S}_h^\epsilon w)(t) = h\sum_{k=0}^{\lfloor T/h\rfloor}\int_0^t \delta^h(t-\tau)\delta^\epsilon(\tau-kh)w(\tau)\,d\tau.$$

We proceed with the assumption that $t\in[lh,\,(l+1)h)$ where $l\geqslant 1$; we deal with the $t\in[0,h)$ case later. Now, the function $\delta^h(t-\tau)\delta^\epsilon(\tau-kh)$ is zero outside the interval $[(l-1)h,(l+1)h\,)\cap[kh,\,kh+\epsilon)$.

So,

$$\begin{aligned}(\hat{H}_h\widehat{S}_h^\epsilon w)(t) &= h\sum_{k=l-1}^{l}\int_0^t \delta^h(t-\tau)\delta^\epsilon(\tau-kh)w(\tau)\,d\tau\\ &= \int_{t-h}^t \delta^h(t-\tau)\delta^\epsilon(\tau-(l-1)h)w(\tau)\,d\tau\\ &\qquad\qquad + \int_{lh}^{lh+\epsilon}\delta^h(t-\tau)\delta^\epsilon(\tau-lh)w(\tau)\,d\tau.\end{aligned}$$

For sufficiently small ϵ the first term is zero because $\delta^\epsilon(\tau-(l-1)h)$ becomes zero on the interval $[t-h,t)$; also for sufficiently small ϵ we have

$\delta^h(t-\tau) = 1/h$ on the interval $[kh,\, kh+\epsilon)$. Therefore, the definition of δ^ϵ yields from above

$$\lim_{\epsilon \to 0} (\hat{H}_h \widehat{S}^\epsilon_h w)(t) = \lim_{\epsilon \to 0} 1/\epsilon \int_{lh}^{lh+\epsilon} w(\tau)\, d\tau = w(lh),$$

where the RHS follows because w is continuous. We can use the same argument, with only cosmetic modifications, to also show that for $t \in [0, h)$ we get $\lim_{\epsilon\to 0}(\hat{H}_h \widehat{S}^\epsilon_h w)(t) = w(0)$.

Define the function $w^0_h(t) := \lim_{\epsilon\to 0}(\hat{H}_h \widehat{S}^\epsilon_h w)(t)$ for each $0 \leqslant t < T$, which we have shown is constant and equal to $w(kh)$ on each interval $[kh,\, (k+1)h\,)$. Clearly, since $w(t)$ is uniformly continuous on $[0, T)$ we have $\lim_{h\to 0} \|w - w^0_h\|_2 = 0$, which is the limit required. ■

Lemma 32 *Suppose $u \in L_2[0, T)$ and $w(t)$ is a uniformly continuous function on the interval $[0, T)$. Then*

$$\lim_{n\to\infty} \lim_{\epsilon\to 0} \|U \hat{H}_{\frac{T}{n}} \widehat{S}^\epsilon_{\frac{T}{n}} w - \Pi_T \Lambda^{-1}_{\frac{T}{n}} \pi^*_{n-1} \tilde{U}_{\frac{T}{n}} \bar{w}^n\|_2 = 0,$$

where $\tilde{U}_h$ is defined from $\tilde{u} = \pi_{n-1}\Lambda^{-1}_{\frac{T}{n}} \Pi^*_T u$ as in (4), and $\bar{w}^n = h \cdot (w(0), \ldots, w(\,(n-1)\frac{T}{n})\,)$.

Proof First apply Lemma 27 to get

$$U \hat{H}_{\frac{T}{n}} \widehat{S}^\epsilon_{\frac{T}{n}} w = \hat{H}_{\frac{T}{n}} U \widehat{S}^\epsilon_{\frac{T}{n}} w.$$

Hence, from the same steps that showed (47) in the proof of Lemma 30 we have

$$\begin{aligned}
\lim_{\epsilon\to 0} U \widehat{S}^\epsilon_{\frac{T}{n}} w &= h \sum_{k=0}^{n-1} w(k\tfrac{T}{n}) \hat{H}_{\frac{T}{n}} u_{(k\frac{T}{n})} \\
&= h \sum_{k=0}^{n-1} w(k\tfrac{T}{n}) u_{(k\frac{T}{n})} + h \sum_{k=0}^{n-1} w(k\tfrac{T}{n}) \{\hat{H}_{\frac{T}{n}} u_{(k\frac{T}{n})} - u_{(k\frac{T}{n})}\} \\
&= \Pi_T \Lambda^{-1}_{\frac{T}{n}} \pi^*_{n-1} \tilde{U}_{\frac{T}{n}} \bar{w}^n + h \sum_{k=0}^{n-1} w(k\tfrac{T}{n}) \{\hat{H}_{\frac{T}{n}} u_{(k\frac{T}{n})} - u_{(k\frac{T}{n})}\}
\end{aligned} \tag{48}$$

Now, concentrating on the second RHS term we see that

$$\begin{aligned}\|h\sum_{k=0}^{n-1} w(k\tfrac{T}{n})\{\hat{H}_{\frac{T}{n}} u_{(k\frac{T}{n})} - u_{(k\frac{T}{n})}\}\|_2 &\leqslant h\sum_{k=0}^{n-1} |w(k\tfrac{T}{n})|\, \|\hat{H}_{\frac{T}{n}} u_{(k\frac{T}{n})} - u_{(k\frac{T}{n})}\|_2 \\ &\leqslant h\, e_{\frac{T}{n}} \sum_{k=0}^{n-1} w(k\tfrac{T}{n}),\end{aligned}$$

where $e_{\frac{T}{n}}$ is defined as in Lemma 29. Hence, above we have

$$\lim_{n\to\infty} \text{LHS} \leqslant (\lim_{n\to\infty} e_{\frac{T}{n}}) \int_0^T |w(\tau)|\, d\tau = 0.$$

Applying this fact to (48) proves the claim. ∎

Lemma 33 *Suppose $u \in L_2[0,T)$ and $w(t)$ is a uniformly continuous function on the interval $[0,T)$. Then*

$$\lim_{n\to\infty} \|Uw - \Pi_T \Lambda_{\frac{T}{n}}^{-1} \pi_{n-1}^* \tilde{U}_{\frac{T}{n}} \bar{w}^n\|_2 = 0,$$

where $\tilde{U}_h$is defined from $\tilde{u} = \pi_{n-1}\Lambda_{\frac{T}{n}}^{-1}\Pi_T^* u$ as in (4), and
$\bar{w}^n = h \cdot (w(0), \ldots,\, w(\,(n-1)\frac{T}{n})\,)$.

Proof Given $\epsilon > 0$ the following inequality holds for each n:

$$\|U\|\, \|(I - \hat{H}_{\frac{T}{n}} \widehat{S}^{\epsilon}_{\frac{T}{n}})w\|_2 + \|U\hat{H}_{\frac{T}{n}} \widehat{S}^{\epsilon}_{\frac{T}{n}} w - \Pi_T \Lambda_{\frac{T}{n}}^{-1} \pi_{n-1}^* \tilde{U}_{\frac{T}{n}} \bar{w}^n\| \geqslant \|Uw - \Pi_T \Lambda_{\frac{T}{n}}^{-1} \pi_{n-1}^* \tilde{U}_{\frac{T}{n}} \bar{w}^n\|_2.$$

Invoking Lemmas 31 and 32 we have $\lim_{n\to\infty} \lim_{\epsilon\to 0}$LHS=0, and so $\lim_{n\to\infty}$RHS= 0. ∎

At last we can prove Lemma 8:

Proof of Lemma 8

Part (i): Suppose that $\bar{w}^n \in \mathcal{R}^n$, and let $w(t)$ be a uniformly continuous function on the interval $[0,T)$ that satisfies $w(kh) = \bar{w}^n_k$ for $0 \leqslant k < n-1$. Then by Lemma 30 we have that

$$\lim_{\epsilon\to 0} \{\, \langle U\widehat{S}^{\epsilon}_h w,\, U\widehat{S}^{\epsilon}_h w\rangle - \langle V\widehat{S}^{\epsilon}_h w,\, V\widehat{S}^{\epsilon}_h w\rangle \,\} = \langle \tilde{U}_h \bar{w}^n,\, \tilde{U}_h \bar{w}^n\rangle - \langle \tilde{V}_h \bar{w}^n,\, \tilde{V}_h \bar{w}^n\rangle,$$

where we have used the fact that $\pi_{n-1}(\Lambda_h^{-1})^*\Pi_T^*\Pi_T\Lambda_h^{-1}\pi_{n-1}^* = I$. For each ϵ, by assumption, $\langle U\widehat{S}_h^\epsilon w,\, U\widehat{S}_h^\epsilon w\rangle - \langle V\widehat{S}_h^\epsilon w,\, V\widehat{S}_h^\epsilon w\rangle \} \geqslant 0$, and therefore above the RHS$\geqslant 0$.

Part (ii): Suppose that $V^*V \leqslant U^*U$ is *not* satisfied: then there exists a function $w \in L_2[0,T)$ so that

$$\langle Vw,\, Vw\rangle > \langle Uw,\, Uw\rangle.$$

Without loss of generality we may assume that w is a uniformly continuous function, since the uniformly continuous functions are dense in $L_2[0,T)$. Applying Lemma 33 we therefore have that for sufficiently large n,

$$\langle \tilde{V}_{\frac{T}{n}}\bar{w}^n,\, \tilde{V}_{\frac{T}{n}}\bar{w}^n\rangle \geqslant \langle \tilde{U}_{\frac{T}{n}}\bar{w}^n,\, \tilde{U}_{\frac{T}{n}}\bar{w}^n\rangle,$$

where we have again used the fact $\pi_{n-1}(\Lambda_h^{-1})^*\Pi_T^*\Pi_T\Lambda_h^{-1}\pi_{n-1}^* = I$. So, $\tilde{V}_{\frac{T}{n}}^*\tilde{V}_{\frac{T}{n}} \leqslant \tilde{U}_{\frac{T}{n}}^*\tilde{U}_{\frac{T}{n}}$ does not hold for all n, which completes the contrapositive argument. ■

B Operator Calculations

This appendix presents the calculations required to derive the component parts of the representations of $\bar{P}_w$ and $\bar{P}_v$ given in (28) and (22). It is not required that P_z has a state-space representation. However, if this is the case, then the matrix $\tilde{Z}^*\tilde{Z}$ can be calculated via state-space techniques and we present the approach required. The matrix optimization problems arise via isomorphisms between $\mathcal{N}^\perp(\tilde{B})$ and $\mathcal{R}^b$, for each of the operators. We give the means of explicitly calculating the operators which map the signals between these spaces. These are not required for the formulation of the optimization problem, however they are useful if one wishes to calculate the time-domain representations of the internal signals in the system. The calculation methods are similar to those presented by Bamieh and Pearson [29] and we have therefore kept the notation similar.

Consider the positive time operator of interest, $S_hP_w^+ : L_2[0,\infty) \to l_2$ as an LTI system (with state-space realization $A_w \in \mathcal{R}^{a_w\times a_w}$, $B_w \in \mathcal{R}^{a_w\times b_w}$, $C_w \in \mathcal{R}^{c_w\times a_w}$), followed by a sampler, S_h.

The lifted system, $S_hP_w^+\Lambda_h^{-1} : l_2(L_2[0,h)) \to l_2$, has the state space representation given in (15),

$$\begin{aligned} x_{k+1} &= \tilde{A}_w x_k + \tilde{B}_w^+\tilde{w}_k^+(t), \\ y_k &= C_w x_k, \end{aligned}$$

where $x_k \in \mathcal{R}^{a_w}$, $\tilde{w}_k^+(t) \in L_2[0,h)$, and $y_k \in \mathcal{R}^{c_w}$. The operators $\tilde{A}_w$ and $\tilde{B}_w^+$ are given by, $\tilde{A}_w = e^{A_w h}$, and

$$\tilde{B}_w^+ \tilde{w}_k^+(t) = \int_0^h e^{A_w(h-\tau)} B_w \tilde{w}_k^+(\tau)\, d\tau.$$

Formulation of the model validation problem requires finding a matrix, $\bar{B}_w^+ \in \mathcal{R}^{a_w \times b_w}$, satisfying,

$$\tilde{B}_w^+ (\tilde{B}_w^+)^* = \bar{B}_w^+ (\bar{B}_w^+)^*.$$

To calculate $\bar{B}_w^+$, define $X_w^+ = \tilde{B}_w^+ (\tilde{B}_w^+)^*$, and note that

$$X_w^+ = \int_0^h e^{A_w(h-\tau)} B_w B_w^* e^{A_w^*(h-\tau)}\, d\tau.$$

It is a simple matter to verify that $X_w^+ = (X_w^+)^*$ is the solution to the Lyapunov equation,

$$A_w X_w^+ + X_w^+ A_w^* = -(B_w B_w^* - e^{A_w h} B_w B_w^* e^{A_w^* h}).$$

We note that $X_w^+ \in \mathcal{R}^{a_w \times a_w}$ and is of rank b_w (in the case where (A_w,B_w) is controllable). Following the approach of Bamieh and Pearson [29], define Σ_w^+ and T_w^+ by,

$$X_w^+ = (T_w^+)^* \begin{bmatrix} \Sigma_w^+ & 0 \\ 0 & 0 \end{bmatrix} T_w^+,$$

where $T_w^+ (T_w^+)^* = (T_w^+)^* T_w^+ = I$. Then

$$\bar{B}_w^+ = (T_w^+)^* \begin{bmatrix} (\Sigma_w^+)^{1/2} \\ 0 \end{bmatrix}.$$

We can also explicitly consider the operator mapping $\mathcal{R}^{b_w}$ to $\mathcal{N}^\perp(\tilde{B}_w^+)$. Define this as U_w^+ and note that $\bar{B}_w^+ = \tilde{B}_w^+ U_w^+$. Therefore,

$$U_w^+ = (\tilde{B}_w^+)^* (T_w^+)^* \begin{bmatrix} (\Sigma_w^+)^{-1/2} \\ 0 \end{bmatrix} = B_w^* e^{A_w^*(h-t)} (T_w^+)^* \begin{bmatrix} (\Sigma_w^+)^{-1/2} \\ 0 \end{bmatrix}.$$

It is a simple matter to verify that $(U_w^+)^* U_w^+ = I$. This operator can be used to calculate $w^+(t)$ (the part of $w(t)$ on $L_2[0,\infty)$), via,

$$w^+(t) = U_w^+ \bar{w}_k^+, \quad kh \leqslant t < (k+1)h,$$

where $\bar{w}^+$ arises from the optimization problem (Problem 22). The minimum norm $w(t)$ is, in general, discontinuous.

The structure of the $S_h P_v$ operator is identical to the $S_h P_w^+$ operator and the above procedure can be used to obtain an analogous representation for $\tilde{A}_v$, $\bar{B}_v$, and, if necessary, U_v and $v(t)$.

In the case of the negative time operator, P_w^-, U_w^- is defined as mapping $\mathcal{R}^{b_w}$ to $L_2(-\infty, 0)$. This in effect omits the lifting operation, as no sampled data is obtained in negative time. The approach is similar to that for $S_h P_w^+$ illustrated above. Recall the representation for $P_w^- : L_2(-\infty, 0) \to l_2$, presented in (6) and (23) as,

$$\begin{aligned} x_{k+1} &= \tilde{A}_w x_k, \quad x_0 = \tilde{B}_w^- \tilde{w}^-, \\ y_k &= C_w x_k, \end{aligned}$$

where, $\tilde{A}_w = e^{A_w h}$ and $\tilde{B}_w^- : L_2(-\infty, 0) \to \mathcal{R}^{a_w}$ via,

$$\tilde{B}^- \tilde{w}^- = \int_{-\infty}^{0} e^{-A_w \tau} B_w w^-(\tau)\, d\tau.$$

We are required to calculate $\bar{B}_w^-$ satisfying, $\bar{B}_w^-(\bar{B}_w^-)^* = \tilde{B}_w^-(\tilde{B}_w^-)^*$. Analogously to the case for $S_h P_w^+$,

$$X_w^- := \tilde{B}_w^-(\tilde{B}_w^-)^* = \int_{-\infty}^{0} e^{-A_w \tau} B_w B_w^* e^{-A_w^* \tau}\, d\tau,$$

and note that X_w^- satisfies the Lyapunov equation,

$$A_w X_w^- + X_w^- A_w^* = -B_w B_w^*.$$

This can be factorized as,

$$X_w^- = (T_w^-)^* \begin{bmatrix} \Sigma_w^- & 0 \\ 0 & 0 \end{bmatrix} T_w^-,$$

with $(T_w^-)^* T_w^- = T_w^-(T_w^-)^* = I$, giving

$$\bar{B}_w^- = (T_w^-)^* \begin{bmatrix} (\Sigma_w^-)^{1/2} \\ 0 \end{bmatrix}.$$

We can again consider the operator defining the isomorphism between $\mathcal{R}^{b_w}$ and $\mathcal{N}^{\perp}(\tilde{B}_w^-)$. In this case $U_w^- : \mathcal{R}^{b_w} \to L_2(-\infty, 0)$ and $\bar{B}_w^- = \tilde{B}_w^- U_w^-$. Therefore,

$$U_w^- = (\tilde{B}_w^-)^* (T_w^-)^* \begin{bmatrix} (\Sigma_w^-)^{-1/2} \\ 0 \end{bmatrix} = B_w^* e^{-A_w^* t} (T_w^-)^* \begin{bmatrix} (\Sigma_w^-)^{-1/2} \\ 0 \end{bmatrix}.$$

This operator can be used to calculate the negative time portion of $w(t)$ via,

$$w(t) = U_w^- \bar{w}^-, \quad -\infty \leqslant t < 0,$$

where $\bar{w}^-$ arises from the optimization problem (Problem 22).

The matrix optimization problem (Problem 22) required that $\tilde{Z}^* \tilde{Z}$ be calculated from the known (or calculated) signal $z(t)$. In many cases we can use a state-space approach, similar to that given above, to facilitate this calculation. We present the details when P_z has the form of a state-space system following a zero-order hold. The methods given here also give a means of extending the model validation procedure to the case where components of $z(t)$ are unknown. This does not give a convex optimization problem and were therefore do not pursue this any further in this paper.

Applying the lifting operation to output of P_z gives, $\tilde{P}_z := \Lambda_h P_z$, as having the representation,

$$\begin{aligned} x_{k+1} &= e^{A_z h} x_k + \int_0^h e^{A_z \tau} B_z u_k \, d\tau, \\ \tilde{z}_k(t) &= \tilde{C}_z x_k + \tilde{D}_z u_k, \end{aligned}$$

where $u_k \in \mathcal{R}^{b_z}$ and $\tilde{z}_k(t) \in L_2^{c_z}[0, h)$. The operators $\tilde{C}_z$ and $\tilde{D}_z$ are given by,

$$\tilde{C}_z = C_z e^{A_z t},$$

and

$$\tilde{D}_z = D_z + C_z \int_0^t e^{A_z \eta} \, d\eta B_z.$$

Note that we do not require $D_z = 0$. The presence of a hold at the input gives a finite-dimensional range for $\tilde{P}_z$.

This time we note that $\tilde{z}_k(t)$ lies the range of the operator $\left[\, \tilde{C}_z \;\; \tilde{D}_z \, \right]$ which is a finite-dimensional subspace of $L_2[0, h)$. We now establish an isometric isomorphism between this space and $\mathcal{R}^{c_z}$. Define $V_z : \mathcal{R}^{c_z} \rightarrow L_2[0, h)$, with $V_z^* V_z = I$. Now $\bar{P}_z : l_2 \rightarrow l_2$, can be defined as,

$$\bar{P}_z := \tilde{V}_z \tilde{P}_z,$$

where,

$$\tilde{V}_z = \operatorname{diag}(V_z, V_z, \ldots).$$

The discrete time system, $\bar{P}_z$ has following representation.

$$\begin{aligned} x_{k+1} &= e^{A_z h} x_k + \int_0^h e^{A_z \tau} B_z u_k \, d\tau, \\ \hat{z}_k &= V_z^* \tilde{C}_z x_k + V_z^* \tilde{D}_z u_k. \end{aligned}$$

Now $V_z : \mathcal{R}^{c_z} \to \text{Im}\left(\left[\begin{array}{cc} \tilde{C}_z & \tilde{D}_z \end{array}\right]\right)$ and satisfies, $V_z^* V_z = I$. Analogously to the U_w^+ case, define T_z and Σ_z by,

$$\left[\begin{array}{c} \tilde{C}_z^* \\ \tilde{D}_z^* \end{array}\right]\left[\begin{array}{cc} \tilde{C}_z & \tilde{D}_z \end{array}\right] = T_z^* \left[\begin{array}{cc} \Sigma_z & 0 \\ 0 & 0 \end{array}\right] T_z.$$

Defining V_z by,

$$V_z = \left[\begin{array}{cc} \tilde{C}_z & \tilde{D}_z \end{array}\right] T_z^* \left[\begin{array}{c} \Sigma_z^{-1/2} \\ 0 \end{array}\right],$$

gives $V_z^* V_z = I$ as required and allows us to calculate

$$\left[\begin{array}{cc} V_z^* \tilde{C}_z & V_z^* \tilde{D}_z \end{array}\right] = \left[\begin{array}{cc} \Sigma_z^{1/2} & 0 \end{array}\right] T_z.$$

To calculate T_z and Σ_z we proceed as follows. Observe that,

$$\left[\begin{array}{cc} \tilde{C}_z & \tilde{D}_z \end{array}\right] = \left[\begin{array}{cc} C_z & D_z \end{array}\right] e^{\left[\begin{smallmatrix} A_z & B_z \\ 0 & 0 \end{smallmatrix}\right] t},$$

and therefore,

$$\left[\begin{array}{c} \tilde{C}_z^* \\ \tilde{D}_z^* \end{array}\right]\left[\begin{array}{cc} \tilde{C}_z & \tilde{D}_z \end{array}\right] = \int_0^h e^{\left[\begin{smallmatrix} A_z^* & 0 \\ B_z^* & 0 \end{smallmatrix}\right]\tau} \left[\begin{array}{c} C_z^* \\ D_z^* \end{array}\right]\left[\begin{array}{cc} C_z & D_z \end{array}\right] e^{\left[\begin{smallmatrix} A_z & B_z \\ 0 & 0 \end{smallmatrix}\right]\tau} \, d\tau$$

The following useful matrix exponential result is given by Van Loan [43];

$$e^{\left[\begin{smallmatrix} A_1 & B_1 \\ 0 & A_2 \end{smallmatrix}\right] t} = \left[\begin{array}{cc} e^{A_1 t} & \int_0^t e^{A_1 (t-s)} B_1 e^{A_2 s} \, ds \\ 0 & e^{A_2 t} \end{array}\right]. \tag{49}$$

To apply this result, define

$$Q = \left[\begin{array}{c} C_z^* \\ D_z^* \end{array}\right]\left[\begin{array}{cc} C_z & D_z \end{array}\right],$$

and

$$A_3 = \left[\begin{array}{cc} A_z & B_z \\ 0 & 0 \end{array}\right].$$

Now define A_4 from the following calculation;

$$e^{\begin{bmatrix} -A_3^* & Q \\ 0 & A_3 \end{bmatrix} h} = \begin{bmatrix} A_4(1,1) & A_4(1,2) \\ A_4(2,1) & A_4(2,2) \end{bmatrix}.$$

It is simple to show, using (49), that

$$\begin{bmatrix} \tilde{C}_z^* \\ \tilde{D}_z^* \end{bmatrix} \begin{bmatrix} \tilde{C}_z & \tilde{D}_z \end{bmatrix} = A_4(2,2)^* A_4(1,2),$$

and factorizing this gives the required matrices.

Now $\bar{z}$ can be calculated as $\bar{z} = \bar{P}_z u_k$, and $\tilde{Z}^* \tilde{Z}$ is formed from $\bar{z}_k$ as in (4).

C Linear Matrix Inequality Based Optimization Approach

The calculation approach taken here is based on a modified method of centers, described by Boyd and El Ghaoui [44], with additional modifications by Fan and Nekooie [45]. Applying these methods to experimental data leads to large optimization problems. Exploitation of the problem structure is an essential step in making these computations feasible. In this section we outline the algorithmic methods for our particular LMI optimization problem.

Other methods exist for solving such problems, and examples of these are described in [46, 47]. We have chosen to base our approach on the method of centers because of the significant computational advantage arising from the structural form of our problem. A more complete assessment of the relative merits of the various approaches is beyond the scope of this report.

The following optimization problem is considered, which is based on the conditions in Theorem 16. For notational simplicity we will express this in terms of β, where $\beta = \gamma^2$. Furthermore, the notation $\mathcal{T}(v)$ will denote the block Toeplitz matrix formed from the vector, v, as in (4). The optimization problem to be considered is:

$$\hat{\beta} := \inf_{v \in \mathcal{R}^v, w \in \mathcal{R}^w} \beta, \tag{50}$$

subject to the constraints,

$$\begin{bmatrix} \beta Z^* Z & \mathcal{T}(v)^* \\ \mathcal{T}(v) & I \end{bmatrix} > 0, \qquad \begin{bmatrix} \beta & w^* \\ w & I \end{bmatrix} > 0, \quad \text{and} \quad r = R \begin{bmatrix} v \\ w \end{bmatrix}.$$

It is routine to show, using the Schur complement, that the above conditions, with $r = y - S_h P_y u$, are equivalent to conditions a)–c) in Theorem16. The norm of the smallest h-periodic and h-anticipatory perturbation, and unknown disturbance signal, accounting for the datum is $\sqrt{\hat{\beta}}$ $(= \hat{\gamma})$. We can trivially modify this approach to consider either $\|\Delta\|$ or $\|w\|$ fixed.

C.1 Modified Method of Centers Algorithm

In this section we outline the general LMI algorithm that we intend to customize for efficiently solving the above problem. This method based on one that is by now well documented in the literature (see [44] and references therein), and is presented here for easy reference and tutorial value. All solutions to the equality constraint can be expressed as,

$$\begin{bmatrix} v \\ w \end{bmatrix} = \begin{bmatrix} v_0 \\ w_0 \end{bmatrix} + \begin{bmatrix} N_v \\ N_w \end{bmatrix} x, \quad x \in \mathcal{R}^{n_x}, \tag{51}$$

where $[v_0^* \; w_0^*]^*$ is any particular solution and $[N_v^* \; N_w^*]^*$ spans the kernel of R. The constraints can now be expressed as an LMI in the variable x;

$$F(\beta, x) = F_0(\beta) + \sum_{i=1}^{n_x} x_i \, F_i,$$

where x_i denotes the ith component of x. The matrix $F_0(\beta)$ is affine in β and is given by,

$$F_0(\beta) = \text{diag}(F_{v0}, F_{w0}) = \text{diag}\left(\begin{bmatrix} \beta Z^* Z & \mathcal{T}(v_0) \\ \mathcal{T}(v_0) & I \end{bmatrix}, \begin{bmatrix} \beta & w_0^* \\ w_0 & I \end{bmatrix} \right). \tag{52}$$

The matrices F_i are constant,

$$F_i = \text{diag}(F_{vi}, F_{wi}) = \text{diag}\left(\begin{bmatrix} 0 & \mathcal{T}(N_{vi})^* \\ \mathcal{T}(N_{vi}) & 0 \end{bmatrix}, \begin{bmatrix} 0 & N_{wi}^* \\ N_{wi} & 0 \end{bmatrix} \right), \tag{53}$$

where N_{vi} and N_{wi} are the ith columns of N_v and N_w respectively. We will denote the set of (β,x) such that $F(\beta, x) > 0$, by $\mathcal{X}$. The boundary of this set is denoted by $\partial\mathcal{X}$.

We now consider the following, relatively standard, barrier function,

$$\phi(\beta, x) := \begin{cases} -\log\det F(x, \beta) & \text{if } (\beta, x) \in \mathcal{X} \\ \infty & \text{otherwise} \end{cases}.$$

For $\beta > \hat{\beta}$, $\phi(x, \beta)$ is analytic and strictly convex in x [44]. The analytic center of the set $\mathcal{X}$ is denoted here by $x(\beta)$ and is the unique minimizer for the optimization problem,

$$x(\beta) := \arg \min_{x \in \mathcal{R}^{n_x}} \phi(\beta, x).$$

Calculation of the analytic center is accomplished via Newton's method.

Algorithm 34 (Newton's method, Nesterov & Nemirovskii step size)

Initialize with x^0 such that $(\beta, x^0) \in \mathcal{X}$.

i) Calculate $g(\beta, x^j)$, the gradient of $\phi(\beta, x)$ with respect to x, at $x = x^j$.

ii) Calculate $H(\beta, x^j)$, the Hessian of $\phi(\beta, x)$.

iii) Calculate the Newton step, x_s^j, as the solution to $H(\beta, x^j)\, x_s^j = -g(\beta, x^j)$.

iii) Calculate the Newton decrement, $\delta^j = \sqrt{g(x^j)^* x_s^j}$.

iv) Update x by $x^{j+1} = x^j - \alpha^j x_s^j$, where the step size, α^j, is given by,

$$\alpha^j = \begin{cases} 1 & \text{if } \delta^j \leqslant 0.25 \\ 1/(1+\delta^j) & \text{otherwise} \end{cases}$$

v) Go to step i).

The convergence of this algorithm is proven in Nesterov and Nemirovskii [40]. The computation time is dominated by the calculation of $g(x, \beta)$ and $H(x, \beta)$. In Section C.2 we outline efficient calculation methods for the particular structures arising in (53).

We now give the algorithm to minimize β. In our case this is simpler than that presented in [45].

Algorithm 35 (Modified method of centers)
Select $\theta \in (0, 1)$. Initialize with $(\beta^0, x^0) \in \mathcal{X}$.

i) Calculate the analytic center, $x(\beta^j)$, via Algorithm 34.

ii) Calculate $x'(\beta^j)$, the derivative of the center, $x(\beta^j)$, with respect to β.

iii) Find, via bisection, μ such that $(\hat{x}, \beta^j - \mu) \in \partial\mathcal{X}$, where $\hat{x} = x(\beta^j) - \mu\, x'(\beta^j)$.

iv) Update x by $x^{j+1} = \theta\, x^j + (1-\theta)\hat{x}$.

v) Update β by $\beta^{j+1} = \theta\beta^j + (1-\theta)(\beta^j - \mu)$.

vi) Go to step i).

The inclusion of the $\mu x^*(x^j)$ term is due to Fan and Nekooie. The choice of $\theta > 0$ ensures that $(\beta^{j+1}, x^{j+1}) \in \mathcal{X}$. If θ is very small (β^{j+1}, x^{j+1}) is very close to $\partial\mathcal{X}$. Although this reduces the total number of steps in the Algorithm 35, it increases the number of Newton steps required to find $x(\beta^{j+1})$. In the example presented here, $\theta = 0.05$.

C.2 Exploiting Structure in the Calculations

In this section we tailor the above algorithm to solve the optimization in (50), and outline the computational advantages that are gained.

Note that,

$$\phi(\beta, x) = -\log\det(F_v(\beta, x)) - \log(\beta - w^* w),$$

which allows us to consider the gradient and Hessian of the two matrix inequality constraints independently. Define the gradient and Hessian of each of the above two terms by $g_v(\beta, x)$, $H_v(\beta, x)$, and $g_w(\beta, x)$, $H_w(\beta, x)$. Note that

$$g(\beta, x) = g_v(\beta, x) + g_w(\beta, x), \quad \text{and} \quad H(\beta, x) = H_v(\beta, x) + H_w(\beta, x).$$

Now consider the second terms in the above. It is simple to show that,

$$g_w(\beta, x) = \frac{2}{\beta - w^* w} N_w^* w,$$

and

$$H_w(\beta, x) = \frac{2}{\beta - w^* w} N_w^* N_w \; + \; g_2(\beta, x) g_2(\beta, x)^*,$$

where $w = w_0 + N_w\, x$.

The general, component-wise, formulation for $g_v(\beta, x)$ (see [44]) is,

$$g_{vi}(\beta, x) = -\text{trace}\left(L^{-1} F_{vi} \left(L^{-1}\right)^*\right), \quad i = 1, \ldots, n,$$

where L is a lower triangular Cholesky factorization satisfying, $LL^* = F_v(\beta, x)$. In this case $F_{vi} \in \mathcal{R}^{(b_v+1)n \times (b_v+1)n}$ and generally has $n\, b_v$ non-zero elements. However, this can reformulated as,

$$g_v(\beta, x) = N_v^* \hat{g}_v,$$

where, each component of $\hat{g}_v$ is given by,

$$\hat{g}_{vj} = -\text{trace}\left(L^{-1} \begin{bmatrix} 0 & \mathcal{T}(e_j)^* \\ \mathcal{T}(e_j) & 0 \end{bmatrix} \left(L^{-1}\right)^* \right), \quad j = 1, \ldots, b_v,$$

and where e_j denotes a vector with a 1 in the jth position and zeros elsewhere. The computational saving arises from the fact that $\mathcal{T}(e_j)$ has only between one and n non-zero components and this sparsity can be exploited in calculating the trace.

An analogous approach can be employed for the Hessian. Denote the Hessian of $-\log\det(F_v(\beta, x))$, with respect to v by $\hat{H}_v(\beta, x)$. The i, jth component of this is given by,

$$\hat{H}_{vij} = \text{trace}\left(L^{-1} \begin{bmatrix} 0 & \mathcal{T}(e_i)^* \\ \mathcal{T}(e_i) & 0 \end{bmatrix} \left(L^{-1}\right)^* L^{-1} \begin{bmatrix} 0 & \mathcal{T}(e_j)^* \\ \mathcal{T}(e_j) & 0 \end{bmatrix} \left(L^{-1}\right)^* \right).$$

The Hessian, with respect to x, is given by,

$$H_v(\beta, x) = N_v^* \hat{H}_v(\beta, x) N_v.$$

The calculation of the Cholesky factor of $F_v(\beta, x)$, and its inverse, can be further simplified by noting that,

$$F_v(\beta, x)^{-1} = \begin{bmatrix} I & 0 \\ -\mathcal{T}(v) & I \end{bmatrix} \begin{bmatrix} (\beta Z^* Z - \mathcal{T}(v)^* \mathcal{T}(v))^{-1} & 0 \\ 0 & I \end{bmatrix} \begin{bmatrix} I & -\mathcal{T}(v)^* \\ 0 & I \end{bmatrix}.$$

For completeness, we outline how to calculate the additional quantities required to implement Algorithm 35. To find $x'(\beta)$, note that,

$$\frac{d\, g(\beta, x(\beta))}{d\,\beta} = H(\beta, x(\beta))\, x'(\beta) \; + \; g(\beta, x(\beta)).$$

As $x(\beta)$ is the analytic center, $g(\beta, x(\beta)) = 0$. Note that

$$\frac{d\, g(\beta, x(\beta))}{d\,\beta} = \frac{d\, g_v(\beta, x(\beta))}{d\,\beta} + \frac{d\, g_w(\beta, x(\beta))}{d\,\beta},$$

and it is simple to verify that,

$$\frac{d\, g_w(\beta, x(\beta))}{d\,\beta} = \frac{-1}{\beta - w^* w}\, g_w(\beta, x(\beta)).$$

Using the gradient calculation techniques given above, we can again take advantage of a sparse calculation method for the remaining term. Note that,

$$\frac{d\, g_v(\beta, x(\beta))}{d\,\beta} = N_v^* \frac{d\, \hat{g}_v(\beta, x(\beta))}{d\,\beta}.$$

The ith component is given by,

$$\frac{d\, \hat{g}_{vi}(\beta, x(\beta))}{d\,\beta} = \operatorname{trace}\left(L^{-1} \begin{bmatrix} Z^*Z & 0 \\ 0 & 0 \end{bmatrix} \left(L^{-1}\right)^* L^{-1} \begin{bmatrix} 0 & \mathcal{T}(e_i)^* \\ \mathcal{T}(e_i) & 0 \end{bmatrix} \left(L^{-1}\right)^* \right).$$

The fact that both $F_v(\beta, x)$ and $F_w(\beta, x)$ contain no matrices which are a function of both x and β leads to very simple and efficient gradient calculations.

We now discuss the calculation of μ in Algorithm 35. This can be done separately for $F_v(\beta, x)$ and $F_w(\beta, x)$, and the minimum value used in the algorithm. Finding the maximum value of μ for $F_w(\beta, x)$ involves finding the positive root of a scalar quadratic equation. The $F_v(\beta, x)$ case involves solving a generalized eigenvalue problem. In principle bisection is not required although we have found it more numerically stable to use bisection with a eigenvalue positivity test.